

Leveraging machine learning to uncover multi-pathogen infection dynamics across co-distributed frog families

Daniele L. F. Wiley¹, Kadie N. Omlor¹, Ariadna S. Torres López¹, Celina M. Eberle¹, Anna E. Savage², Matthew S. Atkinson² and Lisa N. Barrow¹

¹ Museum of Southwestern Biology, Department of Biology, University of New Mexico, Albuquerque, New Mexico, United States

² Department of Biology, University of Central Florida, Orlando, Florida, United States

ABSTRACT

Background: Amphibians are experiencing substantial declines attributed to emerging pathogens. Efforts to understand what drives patterns of pathogen prevalence and differential responses among species are challenging because numerous factors related to the host, pathogen, and their shared environment can influence infection dynamics. Furthermore, sampling across broad taxonomic and geographic scales to evaluate these factors poses logistical challenges, and interpreting the roles of multiple potentially correlated variables is difficult with traditional statistical approaches. In this study, we leverage frozen tissues stored in natural history collections and machine learning techniques to characterize infection dynamics of three generalist pathogens known to cause mortality in frogs.

Methods: We selected 12 widespread and abundant focal taxa within three ecologically distinct, co-distributed host families (Bufonidae, Hylidae, and Ranidae) and sampled them across the eastern two-thirds of the United States of America. We screened and quantified infection loads *via* quantitative PCR for three major pathogens: the fungal pathogen *Batrachochytrium dendrobatidis* (Bd), double-stranded viruses in the lineage *Ranavirus* (Rv), and the alveolate parasite currently referred to as Amphibian Perkinsa (Pr). We then built balanced random forests (RF) models to predict infection status and intensity based on host taxonomy, age, sex, geography, and environmental variables and to assess relative variable importance across pathogens. Lastly, we used one-way analyses to determine directional relationships and significance of identified predictors.

Results: We found approximately 20% of individuals were infected with at least one pathogen (231 single infections and 25 coinfections). The most prevalent pathogen across all taxonomic groups was Bd (16.9%; 95% CI [14.9–19%]), followed by Rv (4.38%; 95% CI [3.35–5.7%]) and Pr (1.06%; 95% CI [0.618–1.82%]). The highest prevalence and intensity were found in the family Ranidae, which represented 74.3% of all infections, including the majority of Rv infection points, and had significantly higher Bd intensities compared to Bufonidae and Hylidae. Host species and environmental variables related to temperature were key predictors identified in RF models, with differences in importance among pathogens and host families. For Bd and Rv, infected individuals were associated with higher latitudes and cooler, more stable temperatures, while Pr showed trends in the opposite direction. We found no

Submitted 18 October 2024
Accepted 3 January 2025
Published 29 January 2025

Corresponding author
Daniele L. F. Wiley,
dwiley7@unm.edu

Academic editor
Daniel Hughes

Additional Information and
Declarations can be found on
page 21

DOI 10.7717/peerj.18901

© Copyright
2025 Wiley et al.

Distributed under
Creative Commons CC-BY 4.0

OPEN ACCESS

significant differences between sexes, but juvenile frogs had higher Rv prevalence and Bd infection intensity compared to adults. Overall, our study highlights the use of machine learning techniques and a broad sampling strategy for identifying important factors related to infection in multi-host, multi-pathogen systems.

Subjects Biodiversity, Ecology, Data Mining and Machine Learning

Keywords *Batrachochytrium dendrobatidis*, *Ranavirus*, Amphibian Perkinsea, Random forests, Amphibian disease, Bufonidae, Hylidae, Ranidae

INTRODUCTION

In the last century, amphibians have experienced declines and extinctions attributed to a myriad of anthropogenic stressors, including climate change, habitat destruction, and species introductions (Bellard, Genovesi & Jeschke, 2016; Miller et al., 2018; Cordier et al., 2021). These factors have collectively led to classifying 41% of known species as threatened or endangered by the International Union for Conservation of Nature (Luedtke et al., 2023). Investigations following enigmatic declines have further identified the emergence of infectious diseases as a significant contributor to amphibian biodiversity loss (Berger et al., 1998; Smith, Acevedo-Whitehouse & Pedersen, 2009; Scheele et al., 2019; Rollins-Smith, 2020). With the projected increase in infectious disease spread alongside anticipated climatic shifts (Rollins-Smith, 2017; Price et al., 2019), there is a pressing need for continued disease surveillance and assessment of multi-pathogen infection dynamics within host communities.

Across North American frogs, mortality events have been linked to three major pathogens—the aquatic fungus *Batrachochytrium dendrobatidis* (Bd, Scheele et al., 2019), double-stranded viruses in the genus *Ranavirus* (Rv, Miller, Gray & Storfer, 2011), and the protozoan endoparasite known as Amphibian Perkinsea (Pr, Isidoro-Ayza et al., 2017). Since their respective discoveries, research has shown that infection prevalence and impact vary across and within host taxa (e.g., Greenberg, Palen & Mooers, 2017), demographic traits such as age (Humphries et al., 2022) and sex (Adams et al., 2017; Belasen et al., 2019), and environmental conditions related to latitude, elevation, and seasonality (Petersen et al., 2016; Whitfield et al., 2017; Sasso, McCallum & Grogan, 2021). These studies, however, are often limited by reduced taxonomic and geographic breadth and investigate only one pathogen at a time. Standardized screening efforts for multiple pathogens across susceptible host species sampled within the same environments are needed to effectively capture the complex interactions of factors driving infectious disease patterns.

Although Bd, Pr, and Rv can infect a diverse range of host taxa, susceptibility is not uniform across all taxonomic groups (Bancroft et al., 2011) and certain life history traits have been attributed to pathogen-specific infection risk. For example, due to the reliance on water as a mechanism for pathogen spread and persistence, Bd, Pr, and Rv infections are more prevalent in species associated with aquatic habitats (Bd—Greenberg, Palen & Mooers, 2017), such as ephemeral ponds (Rv—Hoverman et al., 2011; Pr—Hartmann et al., 2024). Additionally, variation in infection outcomes across and within species has also been demonstrated both in *ex situ* pathogen challenge experiments (e.g., Bd: Gervasi et al.,

2013; Becker *et al.*, 2014; Rv: Hoverman, Gray & Miller, 2010) and *in situ* community-wide surveys (e.g., Bd: Whitfield *et al.*, 2017). These differences in infection outcome among species may be explained by a combination of ecological and life history traits (Becker *et al.*, 2014), host genetics (Savage, Becker & Zamudio, 2015), immunogenetics (Savage *et al.*, 2019; Trujillo *et al.*, 2021), as well as environmental factors known to impact the host's immune responses (Raffel *et al.*, 2006; Rollins-Smith, 2017), further highlighting the challenges of assessing broad infection dynamics in natural systems.

Additionally, host demographic traits such as age class (reviewed in Humphries *et al.*, 2022) and sex (Adams *et al.*, 2017; Belasen *et al.*, 2019), as well as coinfection with multiple pathogens (Ramsay & Rohr, 2021; Atkinson & Savage, 2023b), can further explain population-level variation in infection dynamics. For example, some studies show that metamorphic and post-metamorphic adult frogs suffer higher mortality rates compared to larvae when infected with Bd (Abu Bakar *et al.*, 2016; Humphries *et al.*, 2024), presumably due to the higher percentage of keratinized skin cells which the fungus uses as its primary resource. In contrast, frogs during their adult life stage tend to have the lowest prevalence of Pr and Rv infection, likely due to the increased competence of the host's immune system after metamorphosis (Gray, Miller & Hoverman, 2009; Karwacki *et al.*, 2018; Karwacki, Martin & Savage, 2021). Moreover, in some species, males exhibit higher Bd prevalence (Adams *et al.*, 2017) and lower Bd survival rates compared to females (Carey *et al.*, 2006), which could be because of differences in behavior related to exposure (e.g., males congregate in water for longer periods during breeding) or physiology (e.g., higher levels of testosterone may suppress immune function). To complicate things even further, harboring multiple pathogens can impact host tolerance to infection (Johnson & Boller, 2011), with coinfections of Bd and Rv resulting in inhibited growth and increased mortality (Ramsay & Rohr, 2021). Due to the context-dependent nature of interactions between host and pathogen dynamics, capturing this broad variation in susceptibility and mortality across communities is challenging and requires extensive surveys to better understand the generality of these patterns.

Environmental variables, including aspects of temperature and precipitation, influence pathogen distributions across susceptible hosts (e.g., Sasso, McCallum & Grogan, 2021). Though Bd and Rv differ in their thermal limits (Longcore, Pessier & Nichols, 1999; Ariel *et al.*, 2009), with Bd being more sensitive to higher temperatures, both pathogens have been reported across much of North America (Peterson & McKenzie, 2014; Bartlett *et al.*, 2021). Pathogen mediated mortality, however, has been strongly associated with temperature seasonality, where Bd and Rv die-off events tend to peak over winter months, at more northern latitudes, and at higher elevations (Bd: Raffel *et al.*, 2013, 2015; Li *et al.*, 2021; Rv: Gray, Miller & Hoverman, 2009; Balseiro *et al.*, 2010; Rollins-Smith, 2017). Little is currently known about the full distribution and limits of Pr, but seasonal outbreaks have been reported in the Southeastern U.S., mirroring conditions related to Bd and Rv mortality events in this region (Karwacki *et al.*, 2018; Atkinson & Savage, 2023b). The overlap in geographic distribution, suitable environmental conditions, and susceptible host species across all three pathogens leads to high potential for pathogen interactions and warrants further study.

One reason for this gap in research is that multi-host, multi-pathogen studies face sampling challenges due to the number of specimens required to detect pathogens and derive meaningful disease patterns (Stallknecht, 2007). Despite targeted research efforts, achieving sufficient taxonomic and geographic coverage is logistically difficult in a single study. Additionally, while less invasive methods like skin swabs are useful in Bd monitoring surveys, particularly of sensitive species, they are often single-use and may be less accurate at detecting low-level infections and other pathogens (Bd: DiRenzo & Campbell Grant, 2019; Rv: Miller, Gray & Storfer, 2011). Natural history collections offer a potential solution and opportunity for wildlife disease studies (Colella *et al.*, 2021; Thompson *et al.*, 2021). Linking pathogen and parasite data with a vouchered host specimen aligns with the FAIR Data Principles (defined in Wilkinson *et al.*, 2016), which aim to increase data Findability, Accessibility, Interoperability, and Reusability. Vouchered samples facilitate extended genomic, physical, and molecular analyses critical to key discoveries in disease studies (Colella *et al.*, 2021; Karwacki, Martin & Savage, 2021). Therefore, integrating natural history collections into the study of amphibian diseases can help address the large-scale data requirements needed to understand multi-pathogen dynamics, while also allowing for future research to more easily expand on previous discoveries.

Even with adequate sampling, disentangling the interconnected traits related to host-pathogen dynamics is challenging with standard linear statistics (O'Brien, Van Riper & Myers, 2009). Given the high correlation and nonlinearity of potential predictor variables (e.g., aspects of geography, temperature, precipitation), one flexible tool to analyze these complex factors is machine learning. Unlike traditional linear models, machine learning is adept at managing large datasets with numerous correlated variables and is frequently employed in bioinformatic applications (Schwalbe & Wahl, 2020). Specifically, random forests (RF) is a machine learning algorithm that integrates multiple decision trees to predict a response based on many selected variables (Breiman, 2001). This approach can identify features important to amphibian host-pathogen dynamics (Bancroft *et al.*, 2011); however, RF is highly sensitive to class imbalance, which is common when handling disease datasets where one response (e.g., either infected or uninfected) is more strongly represented than the other. In such cases, models are built for and prioritize prediction accuracy of majority cases (e.g., uninfected status) while overlooking the minority cases (e.g., infected status). To address this issue, balanced RF techniques, such as building models with random equal sampling of both majority and minority cases through either downsampling the majority class or upsampling the minority class, can be employed as a correction (Chen, Liaw & Breiman, 2004). In this study, we use balanced RF to evaluate the relative importance of host taxonomy, demographic traits, and geographic and environmental factors for predicting pathogen-specific infection status and intensity.

Investigating geographic regions and species with high pathogen occurrence, but relatively low population decline, can provide valuable insights about the implied infection risk of sensitive co-occurring species. Here, we used range-wide comparisons of widespread and abundant frog species sampled across the central and eastern U.S. to characterize infection status and intensity across multiple hosts, pathogens, and

environments. First, we described the prevalence and intensity of Bd, Pr, and Rv infections and coinfections within three anuran families using museum tissue collections, allowing the assessment of differences across host taxonomy and geographic distributions. Second, we applied machine learning to determine which host traits and environmental factors were most important for predicting pathogen infection status. Lastly, we validated our models and further investigated correlation and directional relationship of identified predictors, *i.e.*, host family, species, age, sex, latitude, elevation, and associated temperature and precipitation variables related to pathogen occurrence and infection loads using traditional statistical methods.

MATERIALS AND METHODS

Sampling

We obtained tissue samples through field collections and museum loans (Table S1). Individuals were largely sampled during summer breeding months from 2009–2023 under appropriate state and local permits (see Field Study Permissions below) and were archived at the Museum of Southwestern Biology (MSB), University of New Mexico (UNM).

Post-metamorphic frogs were captured by hand, often along public roadways or near lentic waterways, while tadpoles were collected *via* dipnet. Individuals were either toe clipped and released at the site of capture or euthanized shortly after capture following protocols approved by the UNM Institutional Animal Care and Use Committee (Protocols 20-201006-MC & 23-201375-MC) and Florida State University (FSU) Animal Care and Use Committee (Protocols 1017 & 1313). Specifically, we applied 20% benzocaine to the ventral side of the frog, as described in the Guidelines for Use of Live Amphibians and Reptiles in Field and Laboratory Research (*Herpetological Animal Care and Use Committee (HACC), 2004*). Once the frog was completely unresponsive, we removed the heart as a secondary means of euthanasia. Dissection tools were flame sterilized between individuals, but not between tissue types collected. Tissues (toe, tail, muscle, and/or liver) were preserved either in 95% ethanol or tissue buffer (20% DMSO, 0.25 M EDTA, salt-saturated), or were immediately flash frozen in liquid nitrogen and kept frozen until DNA extraction.

In total, we obtained 1,281 samples from 32 states across the central and eastern U.S. (Fig. 1). Samples were selected to represent three major anuran families (Bufonidae $n = 320$, Hylidae $n = 456$, Ranidae $n = 505$) with four taxa in each family (11 species and one species complex; Fig. 1). Specifically, we targeted common and abundant species with overlapping distributions to facilitate comparisons across families while controlling for geographic and environmental variables.

Molecular methods

Genomic DNA was extracted from tissue samples that consisted of either external only (toe, tail $n = 259$), internal only (liver, muscle $n = 363$), or a combination of both tissue types ($n = 586$; Fig. S1). We note that the use of internal tissues is not recommended for detecting Bd (*World Organisation for Animal Health (WOAH), 2021a*); however, during dissection, Bd zoospores are occasionally transferred from the skin to internal tissues. We therefore expected occasional, but not reliable detection of Bd from internal tissues

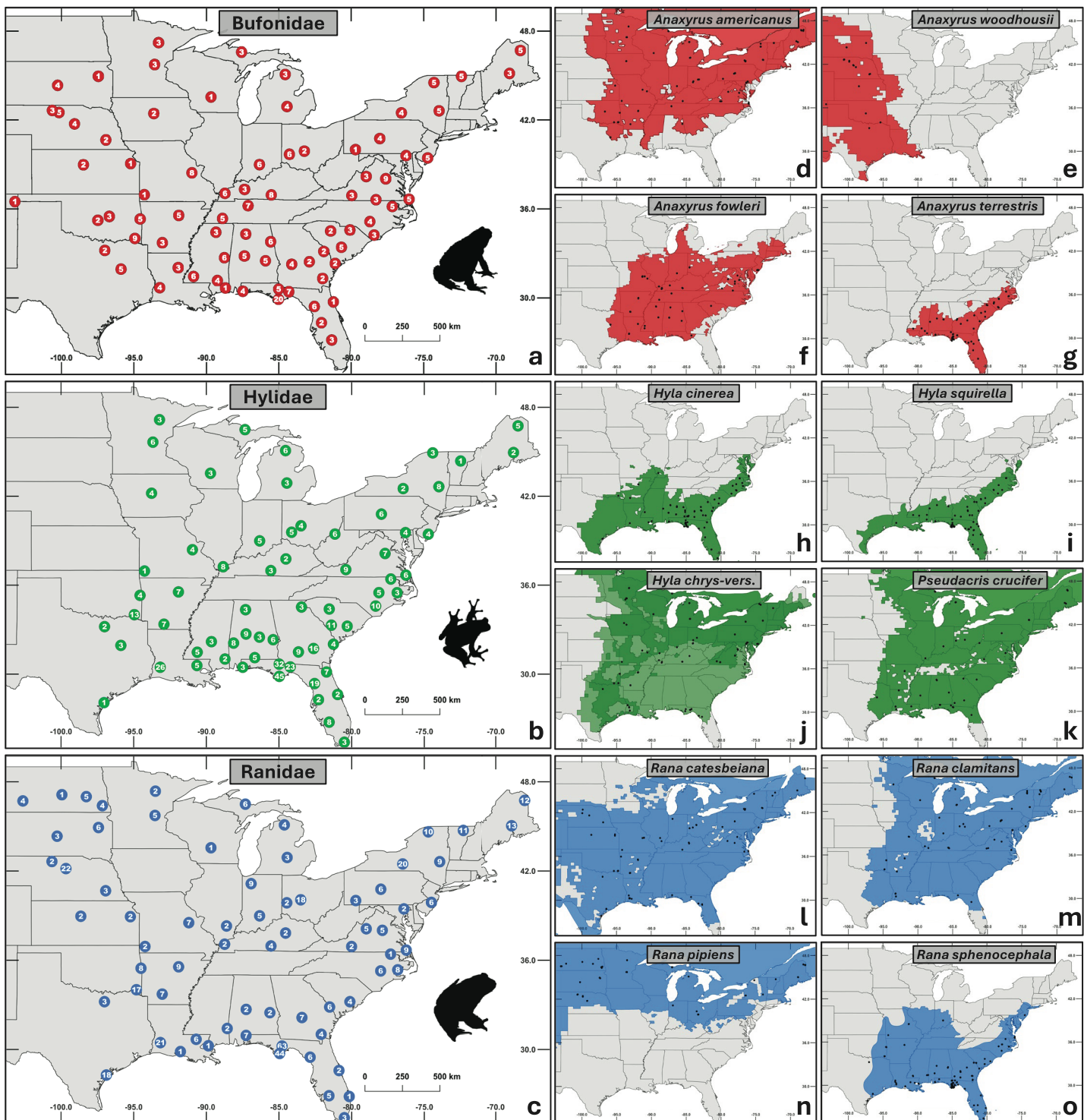


Figure 1 Maps of sampling distribution by taxonomic group. (A–C) Aggregated sampling depth for each family, with the number of individuals sampled shown at each site. (D–O) Species within each family sampled. Black dots represent sampled sites, and the colored regions depict native ranges obtained from the international union for conservation of nature red list (IUCN, 2022). (J) Combined ranges of cryptic species *Hyla chrysoscelis* and *H. versicolor*. Silhouettes of frogs were obtained from phylopic.org.

Full-size DOI: [10.7717/peerj.18901/fig-1](https://doi.org/10.7717/peerj.18901/fig-1)

(demonstrated in a comparison by [Torres López et al., 2024](#)), which is why extractions of these samples were included in select downstream analyses.

We used the E.Z.N.A. Tissue DNA Extraction Kit (Omega Bio-tek, Inc, Norcross, GA, USA) following the manufacturer's recommendations. Whole genomic DNA concentrations were determined using the Broad Range Qubit Assay (Invitrogen, Eugene, OR, USA) and standardized to DNA concentrations of 9–15 ng/μL. Pathogen presence and quantity were determined *via* quantitative PCR (qPCR) following established protocols (Bd—[Boyle et al., 2004](#); Rv—[Allender, Bunick & Mitchell, 2013](#); Pr—[Karwacki et al., 2018](#)). Reactions were prepared in a UV-sterilized, clean air workstation. For each pathogen-specific qPCR, we used 25 μL reaction volumes, each containing 5 μL of extracted DNA template, 2 μL each of 10 μM forward and reverse primers, 5 μL of 1 μM probe (Eurofins Genomics, Louisville, KY, USA), and 8 μL SsoAdvanced Universal Probes Supermix (Bio-Rad, Hercules, CA, USA). Serial dilutions of pathogen-specific gBlocks (idtDNA, Coralville, IA, USA) were mixed with 0.1 ng/μL yeast tRNA carrier (Eurofins Genomics) to prevent small nucleic fragments from binding to the low-bind tubes and were used in duplicate as standards on each plate. Two positive controls (5 μL at 10 ng/μL concentration of known positive samples: Bd—MSB:Herp:104601; Rv—MSB:Herp:104600; Pr—MSB:Herp:104643) and two negative controls (molecular grade water) were included on each plate. Plates were run on a CFX96 Touch Real-Time PCR Detection System (Bio-Rad, Hercules, CA, USA), with cycling conditions of 95 °C for 5 min, followed by 40 cycles of 95 °C for 15 s and either 60 °C for 1 min (Bd/Rv) or 59 °C for 1 min (Pr).

Initial screening included two independent runs on each sample for each pathogen type; samples that tested negative in both runs were deemed uninfected, requiring no further screening. Partial and consistent positives underwent re-testing on two more independent plates to rule out false positives and to obtain final infection intensity values, resulting in at least four independent qPCR runs. Infection intensity values were calculated using the amplification curves (Cq) converted into starting quantities of pathogen DNA (SQ), with averages derived from the final two qPCR runs to account for differences in reagent sensitivity between runs. Individuals testing positive half of the time over the four plates of screening were categorized as “low” infections and included in all prevalence evaluations, but their infection intensity values were unreliable and were not considered in downstream analyses.

Calculating pathogen prevalence and infection loads

Pathogen prevalence was determined by summing the number of individuals found positive for each pathogen within a family, species, age, and sex, divided by the total number of samples within that category ([Tables S2–S4](#)). Because of the relatively low proportion of infected individuals within groups, we calculated 95% binomial confidence intervals using the logit method available in the *binom* package in R ([R Core Team, 2023](#); [Sundar, 2006](#)). All individuals were taxonomically assigned and identified to the species or species complex level (*i.e.*, *Hyla chrysoscelis-versicolor*). Samples lacking age class or sex identification at the time of collection were categorized as an unknown and were excluded from prevalence or infection intensity comparisons for those factors.

Reducing dimensionality of environmental variables

We obtained 11 temperature and nine precipitation bioclimatic variables at 30 s (~1 km²) resolution from the WorldClim 2.1 database, which includes climate data from 1970–2000 (Fick & Hijmans, 2017). Variables were centered, scaled, and reduced *via* principal components analyses (PCAs) using the `prcomp()` function in R, with separate analyses conducted for temperature and precipitation. The first two axes for temperature (hereafter, TPC1-2) explained a combined 88.7% of the variation and the first two axes for precipitation (PPC1-2) explained 95.8% of the variation (Fig. S2). Variable loadings indicated TPC1 primarily represented year-round temperatures, with higher values relating to warmer, more stable overall temperatures, while TPC2 represented mean diurnal temperature ranges, with higher values relating to more extreme daily temperature fluctuations. Similarly, PPC1 described the overall precipitation amount, with higher values indicating wetter conditions, whereas PPC2 represented precipitation variability, with higher values representing more variability in rainfall (Tables S5 and S6).

Identifying factors related to infection status and intensity *via* random forests

We employed the machine learning technique, RF, to identify important predictor variables related to infection status and infection intensity. We created classification models to predict pathogen status (infected or uninfected) for datasets with sufficient infection counts, including models encompassing all frogs (Bd_all: $n = 1,281$, Rv_all: $n = 1,187$) and family-specific models for Bd only (Bd_Bufonidae: $n = 320$, Bd_Hylidae: $n = 456$, Bd_Ranidae: $n = 505$). We also created a Bd infection status model excluding internal only and unknown tissues to investigate the impacts of tissue type on our results (Bd_external: $n = 845$). Additionally, we created an RF regression model for Bd infections ($n = 216$) to examine variables important to infection intensity (average SQ values). Models were created and assessed using the *randomForests* (Liaw & Wiener, 2002) and *caret* (Kuhn, 2008) R packages.

To address the large imbalance between infected and uninfected cases across the data, classification models were first balanced by either downsampling or upsampling. For downsampling, majority cases (uninfected) were randomly subsampled with replacement to equal the number of minority cases (infected). For upsampling, minority cases (infected) were randomly duplicated with replacement to equal the number of majority cases (uninfected). RF models were then optimized to predict both majority and minority cases by using the “strata” and “sampszie” functions to pull equal counts of infected and uninfected cases when creating forests. We assessed model overfitting *via* cross-validation and selected the model with the highest performance without overfitting, ultimately using downsampling for all models.

To further mitigate effects of small sample sizes of infected cases, we employed regularization *via* limited maximum depth by using the optimal `mtry` with the `tuneRF()` function of the *randomForests* package. We also used feature selection methods to reduce over-fitting of the data and determined variables for inclusion in our final classification models by comparing average out-of-bag (OOB) error rates. Cross-validations were

performed using the `predict()` function from the *stats* package (R Core Team, 2023) to create a confusion matrix to assess predictive accuracy. To assess regression models, we used mean squared error and R^2 metrics. Final models were constructed with 2,000 trees and 100 permutations, runs were averaged over 100 iterations, and mean error rates were recorded. Average relative importance for each independent variable in the final model was measured using the `importance()` function and visualized using the *ggplot2* package (Wickham, 2016).

Lastly, we evaluated final model performance, assessed predictive accuracy, and documented misclassification by splitting the data into training (70%) and testing (30%) datasets with equal proportions of positive infections and passed testing data through final models 100 times. We applied cross-validation to the final models to assess performance using the same methods described above.

One-way analyses of infection status and intensity

We used parametric and non-parametric tests *via* the *stats* R package to examine relationships between the potential factors associated with infection prevalence and intensity. We assessed model assumptions using the `plotNormalhistogram()` function in the *rcompanion* package and the `var.test()` function in the *stats* package. To assess differences in infection prevalence among categorical variables such as family, species, age class, sex, and tissue type, we used Pearson's chi-squared tests for each pathogen type. We compared aspects of geography (latitude and elevation) and environmental variables (TPC1-2, PPC1-2) between infected and uninfected frogs using Student's two-tailed t-tests. We performed logistic regressions to examine odds of infection across continuous variables such as latitude, longitude, elevation, TPC1-2, and PPC1-2 using the *stats* package and assessed model assumptions using the *rcompanion* package.

To examine differences in infection intensity between categories (family, species, age class, sex), we performed one-way ANOVAs assuming equal variances or Welch's ANOVAs for tests with unequal variances. When comparing mean infection intensity between two groups (e.g., Rv species infection intensity, age class, and sex), we performed two-tailed Student's t-tests. When significant differences were detected in ANOVA results, *post-hoc* analyses were carried out as follows. For parametric data, multiple two-tailed t-tests with Bonferroni correction or Tukey's Honest Significant Difference tests were employed, while for non-parametric data, Games-Howell *post-hoc* tests were conducted using the *rstatix* package (Kassambara, 2023). Additionally, given the possibility of coinfections acting synergistically to increase negative infection outcomes (reviewed in Herczeg *et al.*, 2021), we also evaluated differences in infection intensity between coinfected individuals and individuals with single infections of each pathogen using two-tailed t-tests. Finally, we performed linear regressions to assess infection intensity across continuous variables such as latitude, longitude, elevation, TPC1-2, and PPC1-2 using the *stats* package and assessed model assumptions using the *erikmisc* package (Erhardt, 2024). All R code and datasets are available from Figshare (<https://doi.org/10.6084/m9.figshare.26849554>), specimens are searchable *via* Arctos (arctos.database.museum; Cicero *et al.*,

2024), and pathogen data are available on the Amphibian Disease Portal (Expedition GUID: <https://n2t.net/ark:/21547/FkC2>).

RESULTS

Pathogen prevalence summary

Approximately 20% ($n = 256$) of the 1,281 individual frogs screened were infected with at least one pathogen, 231 with single infections and 25 with coinfections. We found substantial variation in prevalence among pathogens (Figs. 2 and S3), with Bd exhibiting the highest prevalence (16.9%; 95% CI [14.9–19%]), followed by Rv (4.38%; 95% CI [3.35–5.7%]) and Pr (1.06%; 95% CI [0.618–1.82%]). Significant variation in Bd and Rv infections was evident both between and within family groups (Fig. 2A; Table 1), with Pearson residual scores indicating higher-than-expected counts for both pathogens in the family Ranidae (Fig. S4). For Bd, we found higher counts of infection in the species *R. catesbeiana*, *R. clamitans*, and *R. sphenocephala* (Fig. S5). Within Bufonidae and Hylidae, Bd infections were primarily associated with a single species in each family, namely *A. americanus* and *P. crucifer* (Fig. 2A; Table S2). For Rv, we also observed higher-than-expected counts in Ranidae, specifically *R. catesbeiana* and *R. clamitans* (Table 1, Fig. S5). Pr prevalence was consistently low with no discernable pattern of infection across taxonomic groups.

Rv infection prevalence was notably higher in juveniles compared to adults (Tables 1 and S7). We found no significant difference in pathogen prevalence between sexes for any pathogen (Table S8). For Bd, as expected, there were significant differences based on tissue type, with fewer infections from internal only tissues compared to external and combination tissue types (Table 1; Fig S6; Table S9). When we re-ran Bd analyses excluding internal only tissues, family and species remained significant factors for Bd infection status (Table S10).

Bd coinfections represented more than half of the individuals infected with Pr (7 of 13, or 53%) and about a third of those infected with Rv (18 of 52, or 35%). Whereas only 12% of samples infected with Bd represented a coinfection (25 out of 216).

Infection intensity summary

Overall, infection intensities were low, with the highest values observed in Bd infections (Table S11). Bd and Rv intensity varied significantly among families, with the highest Bd intensity found in Ranidae, followed by Hylidae and Bufonidae (Table 1, Fig. 2B). For Bd, significant differences in infection intensity across families were primarily driven by Ranidae and Bufonidae, while for Rv, differences were driven by Hylidae and Ranidae (Figs. 2B and 2D; Table S11). No clear pattern was found in Pr infection intensities across families due to small sample sizes. Interspecific variation revealed differences in infection intensity among species, with significantly higher Bd intensity in *R. clamitans* compared to *A. americanus*, *R. catesbeiana*, and *R. pipiens* (Fig. 2C; Table S12). Rv intensity was somewhat higher in *R. catesbeiana* than *R. clamitans*, but the difference was not significant (Fig. 2E; Table S12).

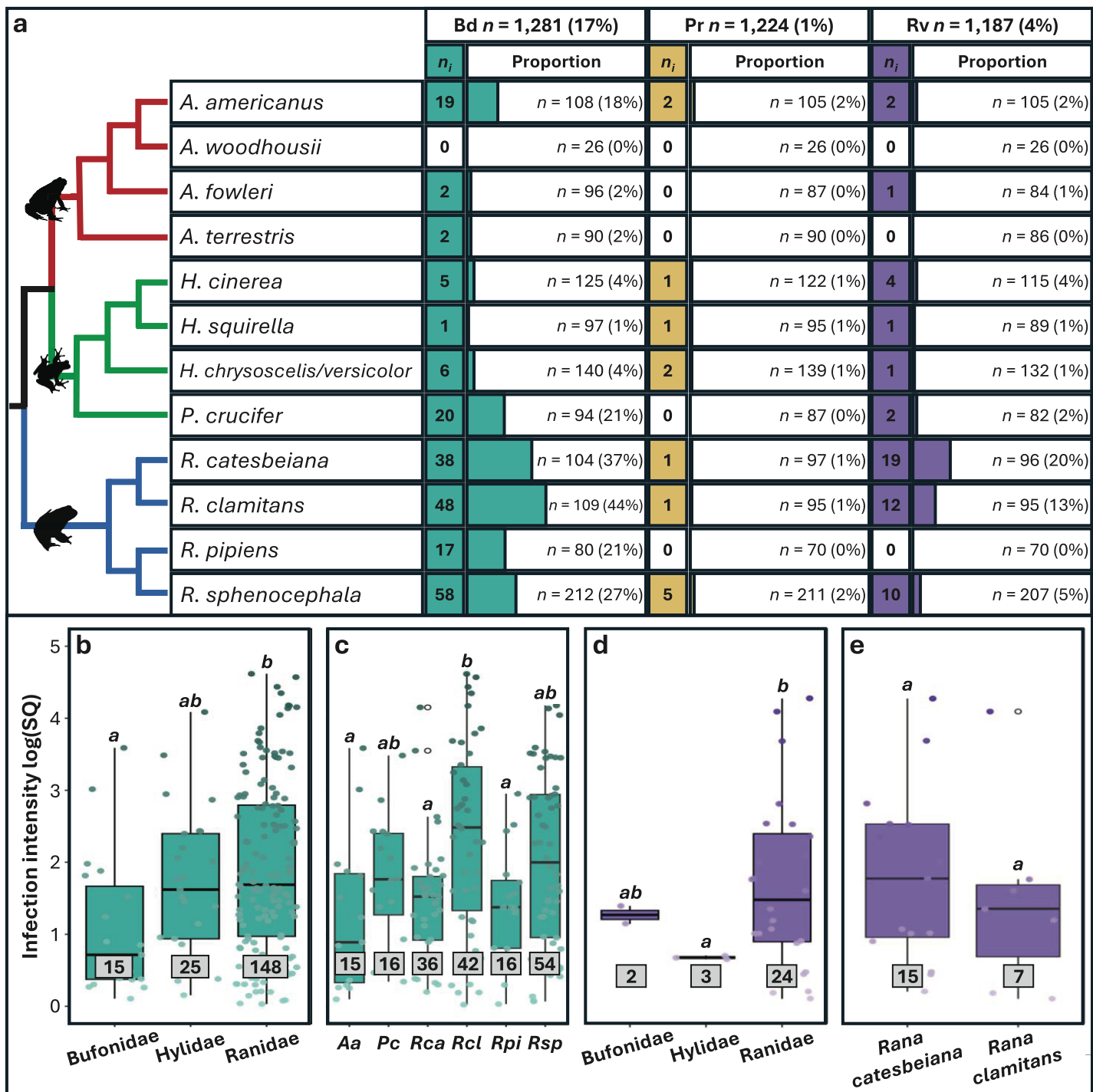


Figure 2 Pathogen prevalence and intensity of infection across host taxonomy. (A) The number (n_i) of individuals infected out of the number sampled (n) and the associated proportion that tested positive for each pathogen (%). Phylogeny is based on relationships obtained from Vertlife.org (Jetz & Pyron, 2018) and edited using FigTree v1.3.1 (Rambaut, 2010). (B-E) Infection intensity values represented by log transformed starting quantities (SQ) for Bd and Rv pathogens with sample sizes in grey boxes. Significant differences ($p < 0.05$) between means for each paired comparison are indicated by differing letters (a, b). Silhouettes of frogs were obtained from phylopic.org. Full-size DOI: 10.7717/peerj.18901/fig-2

Table 1 Summary of parametric and non-parametric statistical analyses.

	<i>Bd</i> status			<i>Pr</i> status			<i>Rv</i> status		
	<i>p</i> value	df	χ^2	<i>p</i> value	df	χ^2	<i>p</i> value	df	χ^2
Family	<0.001	2	134	0.499	2	1.4	<0.001	2	35.8
Species	<0.001	10	179	0.922	6	1.98	<0.001	8	67.8
Age class	0.134	1	2.25	–	–	–	<0.001	1	14.3
Sex	0.918	1	0.011	0.58	1	0.308	0.599	1	0.278
Tissue type	<0.001	1	59.7	0.724	1	0.125	0.874	1	0.025
	<i>p</i> value	df	t stat	<i>p</i> value	df	t stat	<i>p</i> value	df	t stat
Latitude	<0.001 *	289	-4.76	0.005	13.2	3.35	0.002	1,185	-3.15
Log ₁₀ (Elevation)	0.291	1,279	-1.06	0.687	1,222	-0.4	0.195	1,185	-1.3
TPC1	<0.001 *	289	5.29	0.038	12.9	-2.32	0.001	1,185	3.27
TPC2	<0.001	290	4.79	<0.001	13	-6.29	0.354	1,185	0.928
PPC1	0.211	1,279	1.26	0.259	12.9	-1.18	0.386	1,185	0.867
PPC2	<0.001 *	346	-3.36	0.641	1,222	0.466	0.131	1,185	-1.51
	<i>Bd</i> intensity			<i>Pr</i> intensity			<i>Rv</i> intensity		
	<i>p</i> value	df	F/t stat	<i>p</i> value	df	F/t stat	<i>p</i> value	df	F/t stat
Family	0.01	2, 189	(F) 4.69	0.351	2, 7	(F) 1.22	0.035	2, 2.62	(F) 15.5
Species	0.002	5, 57.2	(F) 4.32	–	–	–	0.584	20	(t) 0.566
Age class	0.004	156	(t) -3.63	–	–	–	0.807	21	(t) -0.25
Sex	0.472	105	(t) -0.723	–	–	–	0.222	10	(t) 1.3
Bd & Rv co-infection	0.589	181	(t) -0.541	–	–	–	0.931	27	(t) 0.088
Bd & Pr co-infection	0.552	171	(t) 0.597	0.157	8	(t) 1.57	–	–	–

Note:

Values from tests of pathogen status across 11 factors are shown at the top and tests of pathogen intensity across six factors are shown on the bottom. The test statistic (χ^2 , t stat, or F stat), degrees of freedom (df), and *p* value are shown for Bd, Rv, and Pr. Blank cells indicate tests were not run for that pathogen and factor combination because of insufficient data. Bold text denotes significance (*p* < 0.05). An asterisk (*) denotes variables that are no longer significant when excluding samples derived from internal and unknown tissue types.

We found slightly higher Bd infection intensity in juveniles compared to adults, but there was no significant variation in infection intensity for any pathogen screened related to sex (Fig. S7; Tables S13 and S14). When we re-ran Bd analyses excluding internal only tissues, family and species remained significant for Bd infection intensity, while age class became significant (Table S10). We found no significant differences between Bd infection intensity for individuals with single infections compared to individuals coinfecting with Rv or Pr, nor were there differences in Rv or Pr infection intensity between single infections and coinfections with Bd (Table 1).

RF classification and regression models

The Bd_all RF classification model identified species-level taxonomic rank as the most important factor associated with Bd infection status (Fig. 3A). Overall annual temperature (TPC1), latitude, and daily temperature fluctuations (TPC2) were also important predictors (Fig. 3A). The most important variable differed depending on which infection status class was being considered, with species as the top predictor of uninfected Bd cases

(Fig. 3B), while overall temperature (TPC1) and daily fluctuations (TPC2) showed greater accuracy in predicting infected Bd cases (Fig. 3C). The model exhibited a consistent error rate across classification types at 23.6%, achieving an overall accuracy of 74%. Notably, the model performed similarly at classifying both infected and uninfected cases with sensitivity and specificity scores of 0.70 and 0.79, respectively. The top predictors and model performance for Bd infection status were consistent when we excluded internal only tissues (Fig. S8).

Though there were fewer infection points to sample from, the Rv_all classification model also identified species as the most important predictor of Rv, followed by family, latitude, and TPC1 (Fig. 3D). Species was the most important predictor of uninfected status, while latitude and overall temperature (TPC1) were the top contributing factors to infected Rv cases (Figs. 3E and 3F). The model had an average error rate of 30.2%, with slightly lower error rates for predicting infected status (28.0%) compared to uninfected status (32.5%). Model validation showed moderate accuracy at 71%, with 0.75 sensitivity and 0.71 specificity.

Family-specific RF classification models highlighted differences in top predictors depending on the dataset (Fig. S9). Specifically, for the Bd_Bufonidae and Bd_Hylidae models, species was the most important factor (Figs. S9A–S9F). These results differed from the Bd_Ranidae model, where we observed that species had low importance for predicting infection status and that daily temperature fluctuation (TPC2) was instead the most important factor, followed by latitude and year-round temperature (TPC1; Figs. S9G–S9I). The Bd_Ranidae model had an average error rate of 27.7%, with slightly lower error rates at predicting infected status (27.4%) compared to uninfected (28.0%). Model validation showed moderate accuracy at 70%, with 0.62 sensitivity and 0.74 specificity. For Bd_Bufonidae and Bd_Hylidae, cross-validation revealed higher model accuracy (87% and 89%, respectively), but both models showed signs of model class imbalance, with low sensitivity values (0.5, and 0.55) and high specificity (0.9, 0.91; Figs. S9A and S9D).

The Bd infection intensity RF regression model indicated latitude, overall temperature (TPC1), and precipitation (PPC1) were the top predictors. The model only explained 12.6% of variation, however, with validation showing large mean absolute error (MAE = 1,173) and low R^2 (0.14; Fig. S10).

Geographic and environmental predictors of infection

We observed significant differences in latitude between infected and uninfected individuals across all pathogens (Table 1). For Bd and Rv, infected individuals tended to occur at higher mean latitudes than uninfected (Figs. 4A and 4C), while Pr infections were only found at lower latitudes (Fig. 4B). Within species, the difference in mean latitude between Bd infected and uninfected samples was only statistically significant for *R. clamitans*, with infected samples tending to occur at higher latitudes (Fig. S11). A similar trend was observed in *A. americanus* and *R. catesbeiana*, while *P. crucifer* showed a trend in the opposite direction, with infected individuals tending to occur at lower latitudes.

Elevation and overall precipitation (PPC1) did not exhibit significant differences between infected and uninfected individuals for any pathogen, but differences in the other

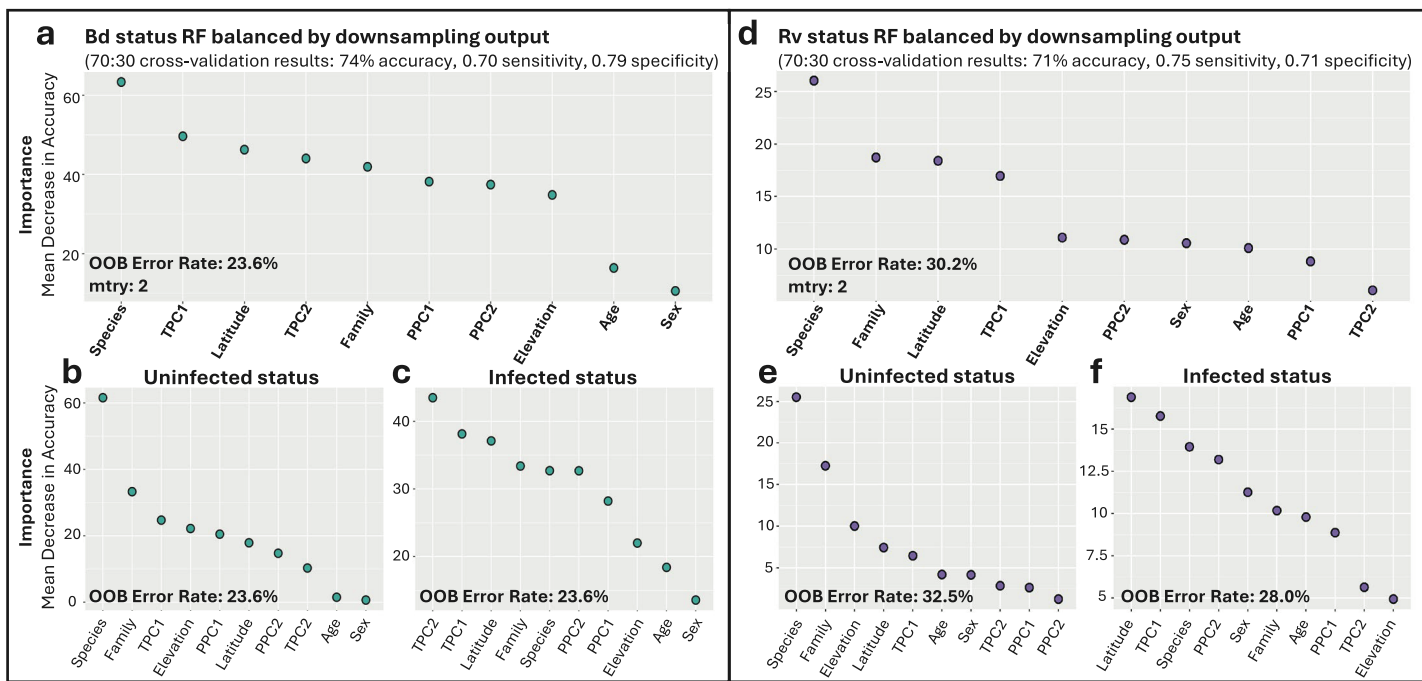


Figure 3 Variable importance for random forests (RF) models of infection status. (A) Overall model of Bd infection status. (B, C) Variables important for Bd uninfected and infected status, respectively. (D) Overall model of Rv infection status. (E, F) Variables important for Rv uninfected and infected status, respectively. For all panels, variable importance is measured as mean decrease in accuracy, averaged across 100 iterations, and ranked from highest (left) to lowest (right) as determined by balanced classification RF analyses. Average out-of-bag (OOB) classification error rates are shown. Predictive accuracy, sensitivity, and specificity values of the final models were derived from cross-validation, with 70% of the data used for training and 30% for testing.

[Full-size](#) DOI: 10.7717/peerj.18901/fig-3

environmental variables (TPC1, TPC2, PPC2) were significant for one or more of the three pathogens (Table 1; Fig. 4). For Bd and Rv, infected individuals were found at lower mean TPC1 than uninfected, suggesting an association with cooler year-round temperatures, while Pr infections were only found at higher TPC1 values (Figs. 4D–4F). For TPC2, Bd infections were associated with lower daily temperature fluctuations, Pr infections with higher daily temperature fluctuations, while the differences between infected and uninfected individuals were not significant for Rv (Figs. 4G–4I). PPC2 only differed for Bd, with slightly higher mean values for infected individuals compared to uninfected (Figs. 4J–4L), indicating Bd infections were associated with higher variability in rainfall. When we re-ran Bd analyses excluding internal only tissues, only differences in TPC2 remained significant (Table S10).

No significant relationships were identified between infection intensity and geographic and environmental factors for any pathogen, but there was a trend of higher infection intensities associated with lower TPC2, which only increased in significance once we removed internal-only samples.

DISCUSSION

Our study design enabled comparisons of infection dynamics across multiple pathogens infecting widespread, co-distributed host taxa, while accounting for geographic and environmental variation. Through this design, we detected different infection patterns

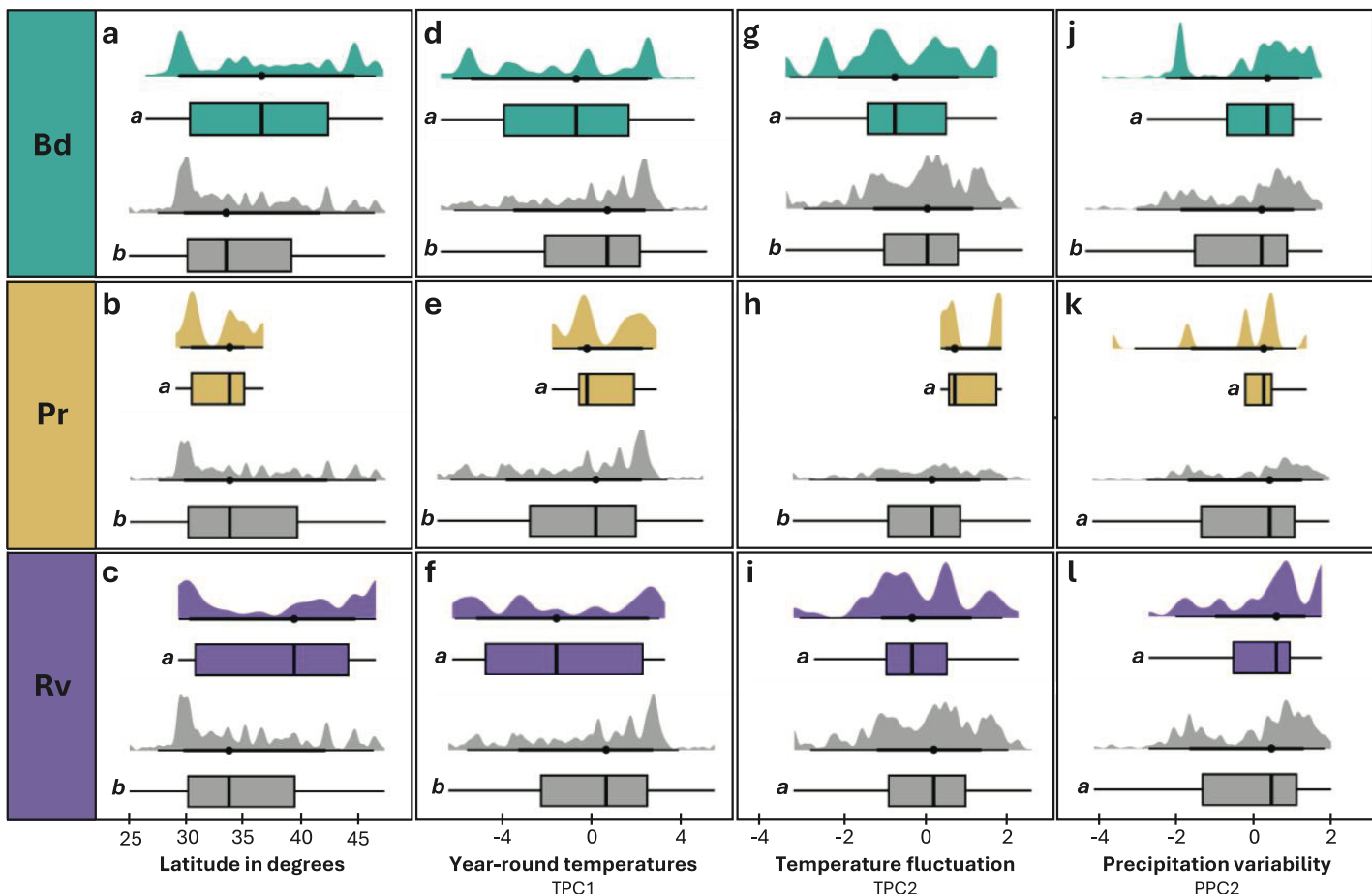


Figure 4 Distribution of latitude and environmental variables across infected and uninfected groups. (A, D, G, J) Individuals tested for Bd and found to be infected (teal) or uninfected (grey). (B, E, H, K) Individuals tested for Pr and found to be infected (tan) or uninfected (grey). (C, F, I, L) Individuals tested for Rv and found to be infected (purple) or uninfected (grey). Distribution of latitude in degrees (A–C), TPC1 (D–F), TPC2 (G–I), and PPC2 (J–L) for infected and uninfected individuals. Significant differences ($p < 0.05$) between means for each paired comparison are indicated by differing letters (a, b).

Full-size DOI: 10.7717/peerj.18901/fig-4

across pathogens, temperature conditions, host taxonomy, and age groups of frogs distributed throughout the central and eastern United States. Even though our study did not sample across seasons, which are known to impact amphibian pathogen dynamics (Duffus *et al.*, 2015; Sasso, McCallum & Grogan, 2021; Atkinson & Savage, 2023b), we were able to capture significant prevalence of amphibian pathogens across this region. We observed widespread Bd infections at low relative intensities across 29 states, supporting the idea that this pathogen is endemic throughout much of this region. We also found that coinfections accounted for more than half of Pr and a third of Rv infections, despite these pathogens typically affecting only larval stages. This suggests that coinfections in adults may play a role in altering susceptibility to pathogens that usually target earlier life stages. In our dataset, individuals infected with Bd and Rv were associated with higher latitudes with lower, more stable overall temperatures, while Pr infections were limited to southern latitudes with increased daily temperature fluctuations, though we note that additional Pr sampling is needed.

Our balanced RF models successfully identified factors important to Bd and Rv infection status. Specifically, each model determined host species as the top predictor with ~70% accuracy, suggesting other factors not captured here are also important in predicting infection status. Broadly speaking, species in the family Ranidae, especially *Rana catesbeiana* and *R. clamitans*, harbored the majority of Bd and Rv infections, adding to the mounting evidence that these species act as potential pathogen reservoirs in this region. Furthermore, we detected higher Rv prevalence and Bd infection intensity in juvenile frogs compared to adults. These findings underscore the complex interplay between host traits, environmental conditions, and pathogen dynamics in shaping infection patterns across this region. We examine these results in relation to previous amphibian pathogen research, discuss sampling limitations, and highlight the challenges and advances that machine learning can provide to large-scale wildlife disease research in the sections below.

Prevalence and geographic distribution vary among pathogens

Batrachochytrium dendrobatidis (Bd)—Our survey is consistent with previous reports (Li *et al.*, 2021), distribution models (Rödder, Schulte & Toledo, 2013; Olson *et al.*, 2021), and public database counts (<https://amphibiandisease.org>; Koo *et al.*, 2021) that indicate the widespread occurrence of Bd across much of the central and eastern United States. We found at least one frog infected with Bd in 29 of the 32 states screened, reinforcing the conclusion that Bd is likely endemic throughout much of this region (Longcore *et al.*, 2007). We also note that northern states such as Maine, Vermont, and Indiana exhibited the highest proportion of Bd infections, with nearly half of all frogs screened testing positive. This high relative prevalence at higher latitudes could be explained by lower overall summer temperatures, which support fungal growth while limiting exposure to above-optimal temperatures that slow disease progression (Lindauer, Maler & Voyles, 2020). Similar patterns have been observed across the U.S. (Petersen *et al.*, 2016; Sonn, Utz & Richards-Zawacki, 2019; Belasen *et al.*, 2024) and Australia (Kriger, Pereoglou & Hero, 2007). However, it is important to acknowledge that our assessment likely underestimates the prevalence of Bd within southeastern regions since many of these samples were derived from internal tissues (e.g., liver, muscle) which are not reliable when screening for Bd (Fig. S1; World Organisation for Animal Health (WOAH), 2021a).

When we excluded samples derived from internal and unknown tissue types, TPC2 (corresponding to mean diurnal temperature range) remained significantly correlated with Bd prevalence. Experimental studies have shown reduced growth and reproduction in Bd when exposed to heat pulses compared to constant temperature treatments (Greenspan *et al.*, 2017; Lindauer, Maler & Voyles, 2020). Likewise, our results suggest that areas with more stable daily temperatures—such as humid, temperate regions near bodies of water—may serve as important refugia for Bd, while more fluctuations in daily temperatures result in decreased pathogen prevalence. Although extensive research has examined climate in relation to Bd infection patterns (e.g., reviewed in Sasso, McCallum & Grogan, 2021), the effect of daily temperature fluctuations in relation to pathogen prevalence and distribution is underreported.

Amphibian Perkinsea (*Pr*)—Our results support three key insights regarding the distribution of *Pr*. First, our study suggests the current known distribution of *Pr* is likely underestimated, as we document novel infections in Missouri and Oklahoma (Isidoro-Ayza *et al.*, 2017; Garner & Ruden, 2019; Midwest Association of Fish and Wildlife Agencies (MAFWA), 2020). Second, the westward range expansion to these states, along with reported mortality events as far north as Wisconsin (Isidoro-Ayza, 2019) and Alaska (Isidoro-Ayza *et al.*, 2017), indicate that *Pr* likely possesses broad climatic tolerances. Although researchers have yet to successfully culture *Pr* in the lab to explore these limits, previous surveys have identified seasonal *Pr* outbreaks throughout the southeastern U.S. (Atkinson & Savage, 2023b). Lastly, the low infection prevalence we document here supports the hypothesis that *Pr* infections are currently localized and rare in adult frogs during summer months, though not impossible (Jones *et al.*, 2012; Karwacki *et al.*, 2018). Nonetheless, with rising concern for species in recent decline, potentially due to the introduction of *Pr*, such as *Rana capito* (Crawford *et al.*, 2022; Devitt *et al.*, 2023) and *Rana sevosa* (Atkinson, 2016), we recommend targeted screening across seasons of abundant co-distributed adult frogs that do not currently show significant population declines, such as *R. catesbeiana*, *R. sphenocephala*, and *R. clamitans*, to assess how these pathogens are potentially spread and maintained in the wild.

Ranavirus (*Rv*)—*Rv* has been documented widely across North America, as shown in the Global Ranavirus Reporting System (brunnerlab.shinyapps.io/GRRS_Interactive/) and subsequent reviews (e.g., Duffus *et al.*, 2015; Brunner *et al.*, 2021). It is important to note that the GRRS database includes reports of infections in both wild and captive frog populations. Therefore, even though *Rv* distributions are recorded widely, some states only have *Rv* outbreaks documented in captivity (Duffus *et al.*, 2015). Our study adds such a novel case of *Rv* infection in wild frogs of Mississippi. The majority of *Rv* infections, however, were detected in northern states such as Maine and New Jersey, where 28% and 13% of individuals tested were found positive, respectively. Similar to *Bd* research, and in line with previous observational studies (e.g., Youker-Smith *et al.*, 2018), we observed significantly higher *Rv* prevalence in areas characterized by cooler year-round temperatures. We note, however, that the higher *Rv* prevalence we found in high-latitude areas may be influenced by the species sampled at northern sites (primarily *Rana catesbeiana* and *R. clamitans*) and the age class of those sampled (many juveniles), both of which are factors that could conceivably correspond with increased infection.

The relatively low overall prevalence of *Pr* and *Rv* in our study was likely influenced by a few factors. First, while both liver and toe clips can reliably detect *Rv* (Torres López *et al.*, 2024) and are recommended diagnostic tissues (World Organisation for Animal Health (WOAH), 2021b), the use of toe clips for *Pr* detection has not yet been validated. Additionally, the absence of larval stages in our sampling likely had a strong impact on prevalence of both *Pr* and *Rv*. While infections (Gray, Miller & Hoverman, 2009; Karwacki *et al.*, 2018) and mortality (Teacher, Cunningham & Garner, 2010) have been documented in adult frogs, mass die-off events for both pathogens primarily occur before and during metamorphosis (*Rv*: Green, Converse & Schrader, 2002; *Pr*: Isidoro-Ayza, 2019). This trend is at least partly explained by the underdeveloped immune response documented in hosts

prior to and during larval development (Gray, Miller & Hoverman, 2009; Miller, Gray & Storfer, 2011; Herczeg *et al.*, 2021), as well as the habitat overlap between these water-borne pathogens and larval stages (Miller, Gray & Storfer, 2011; Itoiz *et al.*, 2022). We did, however, record higher than expected Rv infections in post-metamorphic juvenile frogs compared to adults, perhaps explained by the continued lag in host immune function between metamorphosis and sexual maturity (Rollins-Smith, 1998; Gantress *et al.*, 2003). Lastly, the presence of both Rv and Pr infections in adult frogs in our study may either represent coincidental infections prior to clearance or be related to other mechanisms, such as coinfections, discussed below.

Coinfections account for many cases of rare pathogen infections

Even though we report no significant differences in infection intensity between single and coinfecting individuals, we still document a surprising proportion of coinfections between Bd-Pr and Bd-Rv. This observation, along with findings from other recent multi-pathogen screening efforts (e.g., Landsberg *et al.*, 2013; Karwacki, Martin & Savage, 2021; Atkinson & Savage, 2023b), support the idea that coinfections may facilitate heightened susceptibility in frogs (Herczeg *et al.*, 2021), but more work is needed to understand how these coinfections are affecting seemingly robust species such as *Rana catesbeiana* and *R. clamitans*. Though we did not find coinfections between Pr and Rv, which primarily impact larval stages, infection with Bd may increase susceptibility of adult frogs to Pr and Rv. One concerning aspect of this finding is that given their increased immune function, adults can maintain chronic, low-level infections, thus providing a potential mechanism for pathogen spread and persistence in populations. Further investigation in a controlled setting is warranted to assess how coinfections at different life stages may impact the infection dynamics and outcomes we observe in natural environments and communities.

Infection prevalence differs across host taxonomy

Our study adds to a growing body of research that aims to understand differences in infection prevalence among hosts. Specifically, we found significantly higher Bd and Rv prevalence in four species in the family Ranidae compared to other families (Fig. 2; Fig. S2), while Pr counts were too low to draw significant conclusions. Higher pathogen prevalence in the family Ranidae has been reported from other surveys of wild communities (e.g., Olson *et al.*, 2013; Rothermel *et al.*, 2016; Karwacki *et al.*, 2018), and increased susceptibility has been directly reported in controlled experiments (e.g., Hoverman, Gray & Miller, 2010; Gahl, Longcore & Houlahan, 2012). One potential explanation for increased pathogen prevalence in this family could be proximity and time spent in permanent and semi-permanent breeding ponds that act as pathogen refugia (Hoverman *et al.*, 2011; Greenberg, Palen & Mooers, 2017).

Two species, *Rana catesbeiana* and *R. clamitans*, accounted for 38% of all infected frogs and 64% of all coinfections in our dataset. Both species have been classified as pathogen reservoirs which contribute to the maintenance of Bd and Rv across their native ranges over time (Rothermel *et al.*, 2016; Yap *et al.*, 2018; Brunner *et al.*, 2019; Hoverman, Chislock & Gannon, 2019; Hossack *et al.*, 2023). In addition, the global invasion of

pathogen-positive *R. catesbeiana* has been linked to the spread of both Bd and Rv with primarily negative effects for native species (reviewed in [Atkinson & Savage, 2023a](#)). Other species-level differences observed in our study, such as increased Bd prevalence in *Anaxyrus americanus* and *Pseudacris crucifer* compared to other species in their respective families, also warrants further investigation to identify potential drivers of increased susceptibility outside of primary habitat type. Research into mechanisms of resistance and tolerance (e.g., [Eskew et al., 2015](#)), host-pathogen coevolutionary history (e.g., [Carvalho et al., 2024](#)) and immunogenetic adaptation (e.g., [Trujillo et al., 2021](#)) focused on additional host species could provide further important insights.

Infection intensity varies across host taxonomy and age class

In amphibians, infection intensity serves as a proxy for infection outcomes, with higher pathogen loads often corresponding with increased spread and host mortality ([Vredenburg et al., 2010](#)). Our survey of widespread species that are not currently documented as experiencing pathogen-induced decline, still showed significant associations between infection intensity, host species, and age class. Specifically, we found the highest Bd infection intensities in *Rana clamitans* (Fig. 2B) and significantly higher Bd intensity in juveniles compared to adults (Table S1). The majority of Bd-positive juvenile frogs in our dataset were *R. clamitans*, however, meaning that our data lack the power to distinguish infection intensity variation between age classes and species-level correlates. Importantly, multiple studies have shown that Bd infection intensities increase during winter months ([Savage, Sredl & Zamudio, 2011](#)), which our study also fails to capture. Therefore, more research is needed to assess the differences in Bd intensity across life stages within *R. clamitans* and across seasons to extrapolate the mechanisms responsible for this pattern.

Broadly, age class has been associated with pathogen-induced host mortality, but these results have been mixed. For example, Bd-induced mortality has been documented during metamorphosis ([Humphries et al., 2024](#)) and in juvenile stages ([Abu Bakar et al., 2016](#)), but also the inverse has been recorded, where juveniles harbor lower infection loads compared to adult frogs ([Bradley et al., 2019](#)). This inconsistency demonstrates the contextual nature of infection dynamics, where multiple aspects can influence infection outcomes. Factors such as length of exposure ([Lips, 2016](#); [Bielby et al., 2021](#)), host skin peptides and microbiomes ([Woodhams et al., 2007](#); [Bernardo-Cravo et al., 2020](#)), infection history ([Greenberg, Palen & Mooers, 2017](#)), and phylogenetic constraint ([Hoverman et al., 2011](#); [Longo, Lips & Zamudio, 2023](#)) have all been shown to affect pathogen-specific infection intensities and/or host mortality. Continued work documenting species-specific mechanisms of pathogen tolerance and resistance is needed to better understand the drivers of infection intensity differences and host survival.

Application and limitations of RF models in multi-pathogen dynamics

Our application of balanced RF classification models builds on efforts that have used machine learning to address factors influencing both species-level ([Murray et al., 2013](#)) and site-specific ([Atkinson & Savage, 2023b](#); [Roth, Griffis-Kyle & Barnes, 2024](#)) amphibian infection dynamics. Machine learning techniques have also been applied to examine

projected distributions of Bd in the context of future climate change (Xie, Olson & Blaustein, 2016). We demonstrated the utility of RF models to quickly and efficiently provide valuable insights into the complex patterns encountered in observational disease ecology studies (Cutler *et al.*, 2007). Though there are limitations such as over-fitting due to small sample sizes or amplifying noise in the data rather than true relationships, models built from balanced training datasets with ample sample sizes can achieve moderately low out-of-bag error rates and have high predictive accuracy, specificity, and sensitivity. The application of RF models to other wildlife disease systems such as avian malaria-causing parasites (e.g., Aželytė *et al.*, 2023), *Pseudogymnoascus destructans*, which causes white-nose syndrome in bats, or *Ophidiomyces ophiodiicola*, which causes snake fungal disease, are other promising avenues for discovery.

CONCLUSIONS

Frogs in North America have faced infectious disease pressures from emerging pathogens for over a century (Karwacki, Martin & Savage, 2021). While fine-scale, pathogen-specific research has been essential for understanding the mechanisms driving large-scale infection dynamics, our study underscores the need for multi-pathogen screening efforts to effectively monitor diseases across diverse frog communities. We showed that host species and environmental factors were top predictors of pathogen prevalence, but their relative importance differed among pathogens and host families. Moreover, large-scale studies like ours depend on tissue donations to natural history collections. This practice, along with the deposition of whole specimens, can provide valuable histological and morphometric insights that extend beyond the sample's original research scope, promoting reproducible and extendable science. Lastly, amphibian pathogens present a unique opportunity to develop machine learning models that capture multi-pathogen infection dynamics on a broad scale. The extensive body of research available within this field can enhance model predictions, while the substantial screening efforts can provide ample data to yield valuable insights, when made available *via* public databases. Overall, the multifaceted nature of host-pathogen dynamics poses a challenge to comprehensive, large-scale wildlife disease studies; therefore, future research that embraces data sharing and flexible analytical approaches will pave the way for deeper insights into these complex systems.

ACKNOWLEDGEMENTS

This research is part of the dissertation of DLFW. The authors thank the members of the Amphibian and Reptile Biodiversity Lab for their valuable input on earlier versions of the manuscript and analyses; J. Tom Giermakowski and members of the Division of Amphibians and Reptiles and Mariel Campbell of the Division of Genomic Resources, and the LSU Museum of Natural Science Collection of Genetic Resources, for access to materials and tissues; Melissa Sanchez for laboratory assistance and equipment; and Erik Erhardt in the Department of Mathematics and Statistics and Davorka Gulisija in the Department of Biology for consultation on statistical analyses. We also thank the creators of the original silhouette images: Steven Traver (*Bufo gargarizans gargarizans*), Jose Carlos Arenas-Monroy (*Sarcohyla bistincta*), and Beth Reinke (*Rana temporaria*).

ADDITIONAL INFORMATION AND DECLARATIONS

Funding

This material is based upon work supported by the National Science Foundation Graduate Research Fellowship Program to Daniele L. F. Wiley under Grant No. (2439853) and funding to Lisa N. Barrow from NSF (DEB-2112946) and the University of New Mexico (UNM) Office of the Vice President for Research through a Research Allocations Committee award. Any opinions, findings, and conclusions or recommendations expressed in this material are those of the author(s) and do not necessarily reflect the views of the funders. The funders had no role in study design, data collection and analysis, decision to publish, or preparation of the manuscript.

Grant Disclosures

The following grant information was disclosed by the authors:

National Science Foundation Graduate Research Fellowship Program: 2439853.

NSF: DEB-2112946.

University of New Mexico (UNM) Office of the Vice President for Research through a Research Allocations Committee award.

Competing Interests

The authors declare that they have no competing interests.

Author Contributions

- Daniele L. F. Wiley conceived and designed the experiments, performed the experiments, analyzed the data, prepared figures and/or tables, authored or reviewed drafts of the article, and approved the final draft.
- Kadie N. Omlor performed the experiments, authored or reviewed drafts of the article, and approved the final draft.
- Ariadna S. Torres López performed the experiments, authored or reviewed drafts of the article, and approved the final draft.
- Celina M. Eberle performed the experiments, authored or reviewed drafts of the article, and approved the final draft.
- Anna E. Savage conceived and designed the experiments, authored or reviewed drafts of the article, and approved the final draft.
- Matthew S. Atkinson conceived and designed the experiments, authored or reviewed drafts of the article, and approved the final draft.
- Lisa N. Barrow conceived and designed the experiments, authored or reviewed drafts of the article, and approved the final draft.

Animal Ethics

The following information was supplied relating to ethical approvals (*i.e.*, approving body and any reference numbers):

Florida State University Animal Care and Use Committee; University of New Mexico Institutional Animal Care and Use Committee.

Field Study Permissions

The following information was supplied relating to field study approvals (*i.e.*, approving body and any reference numbers):

Alabama Department of Conservation and Natural Resources; Arkansas Game and Fish Commission; Florida Fish and Wildlife Conservation Commission; Georgia Department of Natural Resources; Iowa Department of Natural Resources; Illinois Department of Natural Resources; Indiana Department of Natural Resources; Kansas Department of Wildlife and Parks; Kentucky Department of Fish and Wildlife Resources; Louisiana Department of Wildlife and Fisheries; Maryland Department of Natural Resources; Maine Department of Inland Fisheries and Wildlife; Michigan Department of Natural Resources; Minnesota Department of Natural Resources; Missouri Department of Conservation; Mississippi Department of Wildlife, Fisheries, and Parks; North Carolina Wildlife Resources Commission; North Dakota Game and Fish Department; Nebraska Game and Parks Commission; New Jersey Division of Fish and Wildlife; New Mexico Department of Game and Fish; New York State Department of Environmental Conservation; Ohio Department of Natural Resources; Oklahoma Department of Wildlife Conservation; Pennsylvania Fish and Boat Commission; South Carolina Department of Natural Resources; State of South Dakota Department of Game, Fish, and Parks; Tennessee Wildlife Resources Agency; Texas Parks and Wildlife; Virginia Department of Wildlife Resources; Vermont Fish and Wildlife Department; Wisconsin Department of Natural Resources.

Data Availability

The following information was supplied regarding data availability:

The data and r-scripts are available at Figshare: Wiley, Daniele (Dani) (2024). CFPCS DATA & R-SCRIPTS. figshare. Dataset. <https://doi.org/10.6084/m9.figshare.26849554.v5>.

The pathogen screening data are available at the Amphibian Disease Portal (GEOME): <https://n2t.net/ark:/21547/R2587>.

Supplemental Information

Supplemental information for this article can be found online at <http://dx.doi.org/10.7717/peerj.18901#supplemental-information>.

REFERENCES

Abu Bakar A, Bower DS, Stockwell MP, Clulow S, Clulow J, Mahony MJ. 2016. Susceptibility to disease varies with ontogeny and immunocompetence in a threatened amphibian. *Oecologia* **181**(4):997–1009 DOI [10.1007/s00442-016-3607-4](https://doi.org/10.1007/s00442-016-3607-4).

Adams AJ, Kupferberg SJ, Wilber MQ, Pessier AP, Grefsrud M, Bobzien S, Vredenburg VT, Briggs CJ. 2017. Extreme drought, host density, sex, and bullfrogs influence fungal pathogen infection in a declining lotic amphibian. *Ecosphere* **8**(3):e01740 DOI [10.1002/ecs2.1740](https://doi.org/10.1002/ecs2.1740).

Allender MC, Bunick D, Mitchell MA. 2013. Development and validation of TaqMan quantitative PCR for detection of frog virus 3-like virus in eastern box turtles (*Terrapene carolina carolina*). *Journal of Virological Methods* **188**(1–2):121–125 DOI [10.1016/j.jviromet.2012.12.012](https://doi.org/10.1016/j.jviromet.2012.12.012).

Ariel E, Nicolajsen N, Christophersen MB, Holopainen R, Tapiovaara H, Bang Jensen B. 2009. Propagation and isolation of ranaviruses in cell culture. *Aquaculture* **294**(3–4):159–164 DOI [10.1016/j.aquaculture.2009.05.019](https://doi.org/10.1016/j.aquaculture.2009.05.019).

Atkinson MS. 2016. The effects of the protist parasite *Dermomycoïdes sp.*, on the dusky gopher frog (*Rana sevosa*) and the southern leopard frog (*Rana sphenocephala*). PhD thesis, Western Carolina University, Cullowhee, NC, USA.

Atkinson MS, Savage AE. 2023a. Invasive amphibians alter host-pathogen interactions with primarily negative outcomes for native species. *Biological Conservation* **286**(3):110310 DOI [10.1016/j.biocon.2023.110310](https://doi.org/10.1016/j.biocon.2023.110310).

Atkinson MS, Savage AE. 2023b. Widespread amphibian *Perkinsea* infections associated with Ranidae hosts, cooler months and *Ranavirus* co-infection. *Journal of Animal Ecology* **92**(9):1856–1868 DOI [10.1111/1365-2656.13977](https://doi.org/10.1111/1365-2656.13977).

Aželytė J, Wu-Chuang A, Maitre A, Žiegytė R, Mateos-Hernández L, Obregón D, Palinauskas V, Cabezas-Cruz A. 2023. Avian malaria parasites modulate gut microbiome assembly in canaries. *Microorganisms* **11**(3):563 DOI [10.3390/microorganisms11030563](https://doi.org/10.3390/microorganisms11030563).

Balseiro A, Dalton KP, Del Cerro A, Márquez I, Parra F, Prieto JM, Casais R. 2010. Outbreak of common midwife toad virus in alpine newts (*Mesotriton alpestris cyreni*) and common midwife toads (*Alytes obstetricans*) in Northern Spain: a comparative pathological study of an emerging ranavirus. *The Veterinary Journal* **186**(2):256–258 DOI [10.1016/j.tvjl.2009.07.038](https://doi.org/10.1016/j.tvjl.2009.07.038).

Bancroft BA, Han BA, Searle CL, Biga LM, Olson DH, Kats LB, Lawler JJ, Blaustein AR. 2011. Species-level correlates of susceptibility to the pathogenic amphibian fungus *Batrachochytrium dendrobatidis* in the United States. *Biodiversity and Conservation* **20**(9):1911–1920 DOI [10.1007/s10531-011-0066-4](https://doi.org/10.1007/s10531-011-0066-4).

Bartlett P, Ward T, Brue D, Carey A, Duffus A. 2021. Ranaviruses in North America: a brief review in wild herpetofauna. *Journal of North American Herpetology* **2021**(2):19–26 DOI [10.17161/jnah.v2021i2.15747](https://doi.org/10.17161/jnah.v2021i2.15747).

Becker CG, Rodriguez D, Toledo LF, Longo AV, Lambertini C, Corrêa DT, Leite DS, Haddad CFB, Zamudio KR. 2014. Partitioning the net effect of host diversity on an emerging amphibian pathogen. *Proceedings of the Royal Society B: Biological Sciences* **281**(1795):20141796 DOI [10.1098/rspb.2014.1796](https://doi.org/10.1098/rspb.2014.1796).

Belasen AM, Bletz MC, Leite DDS, Toledo LF, James TY. 2019. Long-term habitat fragmentation is associated with reduced MHC IIB diversity and increased infections in amphibian hosts. *Frontiers in Ecology and Evolution* **6**:236 DOI [10.3389/fevo.2018.00236](https://doi.org/10.3389/fevo.2018.00236).

Belasen AM, Peek RA, Adams AJ, Russell ID, De León ME, Adams MJ, Bettaso J, Breedveld KGH, Catenazzi A, Dillingham CP, Grear DA, Halstead BJ, Johnson PG, Kleeman PM, Koo MS, Koppl CW, Lauder JD, Padgett-Flohr G, Piovia-Scott J, Pope KL, Vredenburg V, Westphal M, Wiseman K, Kupferberg SJ. 2024. Chytrid infections exhibit historical spread and contemporary seasonality in a declining stream-breeding frog. *Royal Society Open Science* **11**(1):231270 DOI [10.1098/rsos.231270](https://doi.org/10.1098/rsos.231270).

Bellard C, Genovesi P, Jeschke JM. 2016. Global patterns in threats to vertebrates by biological invasions. *Proceedings of the Royal Society B: Biological Sciences* **283**(1823):20152454 DOI [10.1098/rspb.2015.2454](https://doi.org/10.1098/rspb.2015.2454).

Berger L, Speare R, Daszak P, Green DE, Cunningham AA, Goggin CL, Slocombe R, Ragan MA, Hyatt AD, McDonald KR, Hines HB, Lips KR, Marantelli G, Parkes H. 1998. Chytridiomycosis causes amphibian mortality associated with population declines in the rain forests of Australia and Central America. *Proceedings of the National Academy of Sciences of the United States of America* **95**(15):9031–9036 DOI [10.1073/pnas.95.15.9031](https://doi.org/10.1073/pnas.95.15.9031).

Bernardo-Cravo AP, Schmeller DS, Chatzinotas A, Vredenburg VT, Loyau A. 2020. Environmental factors and host microbiomes shape host-pathogen dynamics. *Trends in Parasitology* **36**(7):616–633 DOI [10.1016/j.pt.2020.04.010](https://doi.org/10.1016/j.pt.2020.04.010).

Bielby J, Price SJ, Monsalve-Carcaño C, Bosch J. 2021. Host contribution to parasite persistence is consistent between parasites and over time, but varies spatially. *Ecological Applications* **31**(3):e02256 DOI [10.1002/eaap.2256](https://doi.org/10.1002/eaap.2256).

Boyle D, Olsen DH, Morgan J, Hyatt A. 2004. Rapid quantitative detection of chytridiomycosis (*Batrachochytrium dendrobatidis*) in amphibian samples using real-time Taqman PCR assay. *Diseases of Aquatic Organisms* **60**:141–148 DOI [10.3354/dao060141](https://doi.org/10.3354/dao060141).

Bradley PW, Brawner MD, Raffel TR, Rohr JR, Olson DH, Blaustein AR. 2019. Shifts in temperature influence how *Batrachochytrium dendrobatidis* infects amphibian larvae. *PLOS ONE* **14**(9):e0222237 DOI [10.1371/journal.pone.0222237](https://doi.org/10.1371/journal.pone.0222237).

Breiman L. 2001. Random forests. *Machine Learning* **45**(1):5–32 DOI [10.1023/A:1010933404324](https://doi.org/10.1023/A:1010933404324).

Brunner JL, Olson DH, Gray MJ, Miller DL, Duffus ALJ. 2021. Global patterns of *ranavirus* detections. *FACETS* **6**:912–924 DOI [10.1139/facets-2020-0013](https://doi.org/10.1139/facets-2020-0013).

Brunner JL, Olson AD, Rice JG, Meiners SE, Le Sage MJ, Cundiff JA, Goldberg CS, Pessier AP. 2019. *Ranavirus* infection dynamics and shedding in American bullfrogs: consequences for spread and detection in trade. *Diseases of Aquatic Organisms* **135**(2):135–150 DOI [10.3354/dao03387](https://doi.org/10.3354/dao03387).

Carey C, Bruzgul JE, Livo LJ, Walling ML, Kuehl KA, Dixon BF, Pessier AP, Alford RA, Rogers KB. 2006. Experimental exposures of boreal toads (*Bufo boreas*) to a pathogenic chytrid fungus (*Batrachochytrium dendrobatidis*). *EcoHealth* **3**(1):5–21 DOI [10.1007/s10393-005-0006-4](https://doi.org/10.1007/s10393-005-0006-4).

Carvalho T, Belasen AM, Toledo LF, James TY. 2024. Coevolution of a generalist pathogen with many hosts: the case of the amphibian chytrid *Batrachochytrium dendrobatidis*. *Current Opinion in Microbiology* **78**:102435 DOI [10.1016/j.mib.2024.102435](https://doi.org/10.1016/j.mib.2024.102435).

Chen C, Liaw A, Breiman L. 2004. *Using random forest to learn imbalanced data*. Vol. 110. Berkeley: University of California, 24.

Cicero C, Koo MS, Braker E, Abbott J, Bloom D, Campbell M, Cook JA, Demboski JR, Doll AC, Frederick LM, Linn AJ, Mayfield-Meyer TJ, McDonald DL, Nachman MW, Olson LE, Roberts D, Sikes DS, Witt CC, Wommack EA. 2024. Arctos: community-driven innovations for managing natural and cultural history collections. *PLOS ONE* **19**(5):e0296478 DOI [10.1371/journal.pone.0296478](https://doi.org/10.1371/journal.pone.0296478).

Colella JP, Stephens RB, Campbell ML, Kohli BA, Parsons DJ, Mclean BS. 2021. The open-specimen movement. *BioScience* **71**(4):405–414 DOI [10.1093/biosci/biaa146](https://doi.org/10.1093/biosci/biaa146).

Cordier JM, Aguilar R, Lescano JN, Leynaud GC, Bonino A, Miloch D, Loyola R, Nori J. 2021. A global assessment of amphibian and reptile responses to land-use changes. *Biological Conservation* **253**(80):108863 DOI [10.1016/j.biocon.2020.108863](https://doi.org/10.1016/j.biocon.2020.108863).

Crawford BA, Farmer AL, Enge KM, Greene AH, Diaz L, Maerz JC, Moore CT. 2022. Breeding dynamics of gopher frog metapopulations over 10 years. *Journal of Fish and Wildlife Management* **13**(2):422–436 DOI [10.3996/JFWM-21-076](https://doi.org/10.3996/JFWM-21-076).

Cutler DR, Edwards TC, Beard KH, Cutler A, Hess KT, Gibson J, Lawler JJ. 2007. Random forests for classification in ecology. *Ecology* **88**(11):2783–2792 DOI [10.1890/07-0539.1](https://doi.org/10.1890/07-0539.1).

Devitt TJ, Enge KM, Farmer AL, Beerli P, Richter SC, Hall JG, Lance SL. 2023. Population subdivision in the gopher frog (*Rana capito*) across the fragmented longleaf pine-wiregrass savanna of the southeastern USA. *Diversity* **15**(1):93 DOI [10.3390/d15010093](https://doi.org/10.3390/d15010093).

DiRenzo GV, Campbell Grant EH. 2019. Overview of emerging amphibian pathogens and modeling advances for conservation-related decisions. *Biological Conservation* 236(1827):474–483 DOI 10.1016/j.biocon.2019.05.034.

Duffus ALJ, Waltzek TB, Stöhr AC, Allender MC, Gotesman M, Whittington RJ, Hick P, Hines MK, Marschang RE. 2015. Distribution and host range of *Ranaviruses*. In: Gray MJ, Chinchar VG, eds. *Ranaviruses: Lethal Pathogens of Ectothermic Vertebrates*. Cham: Springer International Publishing, 9–57.

Erhardt E. 2024. Erikmisc: Erik Erhardt's miscellaneous functions for solving complex data analysis workflows. R package version 0.2.12. Available at <https://github.com/erikerhardt/erikmisc>.

Eskew EA, Worth SJ, Foley JE, Todd BD. 2015. American Bullfrogs (*Lithobates catesbeianus*) Resist infection by multiple isolates of *Batrachochytrium dendrobatidis*, including one implicated in wild mass mortality. *EcoHealth* 12(3):513–518 DOI 10.1007/s10393-015-1035-2.

Fick SE, Hijmans RJ. 2017. WorldClim 2: new 1-km spatial resolution climate surfaces for global land areas. *International Journal of Climatology* 37:4302–4315 DOI 10.1002/joc.5086.

Gahl MK, Longcore JE, Houlahan JE. 2012. Varying responses of northeastern North American amphibians to the chytrid pathogen *Batrachochytrium dendrobatidis*. *Conservation Biology* 26(1):135–141 DOI 10.1111/j.1523-1739.2011.01801.x.

Gantress J, Maniero GD, Cohen N, Robert J. 2003. Development and characterization of a model system to study amphibian immune responses to iridoviruses. *Virology* 311(2):254–262 DOI 10.1016/s0042-6822(03)00151-x.

Garner DL, Ruden RM. 2019. Midwest fish and wildlife health committee 2019 status report. Midwest Fish and Wildlife Health Committee. Available at https://www.mafwa.org/wp-content/uploads/2020/11/Part3_4.pdf.

Gervasi S, Gondhalekar C, Olson DH, Blaustein AR. 2013. Host identity matters in the amphibian-*Batrachochytrium dendrobatidis* system: Fine-scale patterns of variation in responses to a multi-host pathogen. *PLOS ONE* 8(1):e54490 DOI 10.1371/journal.pone.0054490.

Gray M, Miller D, Hoverman J. 2009. Ecology and pathology of amphibian *ranaviruses*. *Diseases of Aquatic Organisms* 87:243–266 DOI 10.3354/dao02138.

Green DE, Converse KA, Schrader AK. 2002. Epizootiology of sixty-four amphibian morbidity and mortality events in the USA, 1996–2001. *Annals of the New York Academy of Sciences* 969(1):323–339 DOI 10.1111/j.1749-6632.2002.tb04400.x.

Greenberg DA, Palen WJ, Mooers AØ. 2017. Amphibian species' traits, evolutionary history, and environment predict *Batrachochytrium dendrobatidis* infection patterns, but not extinction risk. *Evolutionary Applications* 10(10):1130–1145 DOI 10.1111/eva.12520.

Greenspan SE, Bower DS, Webb RJ, Roznik EA, Stevenson LA, Berger L, Marantelli G, Pike DA, Schwarzkopf L, Alford RA. 2017. Realistic heat pulses protect frogs from disease under simulated rainforest frog thermal regimes. *Functional Ecology* 31(12):2274–2286 DOI 10.1111/1365-2435.12944.

Hartmann AM, Sash K, Hill EP, Clauch NM, Maddox ML, McGrath-Blaser S, McKinstry CC, Ossiboff RJ, Longo AV. 2024. Partitioning the influence of host specificity in amphibian populations threatened by multiple emerging infectious diseases. *Biological Conservation* 296:110685 DOI 10.1016/j.biocon.2024.110685.

Herczeg D, Ujszegi J, Kásler A, Holly D, Hettyey A. 2021. Host-multiparasite interactions in amphibians: a review. *Parasites & Vectors* 14(1):296 DOI 10.1186/s13071-021-04796-1.

Herpetological Animal Care and Use Committee (HACC). 2004. *Guidelines for use of live amphibians and reptiles in field and laboratory research*. Revised by the Herpetological Animal

Care and Use Committee (HACC) of the American Society of Ichthyologists and Herpetologists. Available at <https://ssarherps.org/wp-content/uploads/2014/07/guidelinesherpsresearch2004.pdf>.

Hossack BR, Oja EB, Owens AK, Hall D, Cobos C, Crawford CL, Goldberg CS, Hedwall S, Howell PE, Lemos-Espinal JA, MacVean SK, McCaffery M, Mosley C, Muths E, Sigafus BH, Sredl MJ, Rorabaugh JC. 2023. Empirical evidence for effects of invasive American bullfrogs on occurrence of native amphibians and emerging pathogens. *Ecology Applications* **33**(2):e2785 DOI [10.1002/eap.2785](https://doi.org/10.1002/eap.2785).

Hoverman JT, Chislock MF, Gannon ME. 2019. *Ranavirus* reservoirs: assemblage of American bullfrog and green frog tadpoles maintains *Ranavirus* infections across multiple seasons. *Herpetological Review* **50**(2):275–278.

Hoverman JT, Gray MJ, Haislip NA, Miller DL. 2011. Phylogeny, life history, and ecology contribute to differences in amphibian susceptibility to *Ranaviruses*. *EcoHealth* **8**(3):301–319 DOI [10.1007/s10393-011-0717-7](https://doi.org/10.1007/s10393-011-0717-7).

Hoverman JT, Gray M, Miller D. 2010. Anuran susceptibilities to *ranaviruses*: role of species identity, exposure route, and a novel virus isolate. *Diseases of Aquatic Organisms* **89**:97–107 DOI [10.3354/dao02200](https://doi.org/10.3354/dao02200).

Humphries JE, Lanctôt CM, McCallum HI, Newell DA, Grogan LF. 2024. Chytridiomycosis causes high amphibian mortality prior to the completion of metamorphosis. *Environmental Research* **247**(4):118249 DOI [10.1016/j.envres.2024.118249](https://doi.org/10.1016/j.envres.2024.118249).

Humphries JE, Lanctôt CM, Robert J, McCallum HI, Newell DA, Grogan LF. 2022. Do immune system changes at metamorphosis predict vulnerability to chytridiomycosis? An update. *Developmental & Comparative Immunology* **136**:104510 DOI [10.1016/j.dci.2022.104510](https://doi.org/10.1016/j.dci.2022.104510).

Isidoro-Ayza M. 2019. Mass mortality of green frog (*Rana clamitans*) tadpoles in Wisconsin, USA, associated with severe infection with the pathogenic *Perkinsea* clade. *Journal of Wildlife Diseases* **55**(1):262–265 DOI [10.7589/2018-02-046](https://doi.org/10.7589/2018-02-046).

Isidoro-Ayza M, Lorch JM, Gear DA, Winzeler M, Calhoun DL, Barichivich WJ. 2017. Pathogenic lineage of *Perkinsea* associated with mass mortality of frogs across the United States. *Scientific Reports* **7**(1):10288 DOI [10.1038/s41598-017-10456-1](https://doi.org/10.1038/s41598-017-10456-1).

Itoïz S, Metz S, Derelle E, Reñé A, Garcés E, Bass D, Soudant P, Chambouvet A. 2022. Emerging parasitic protists: The case of *Perkinsea*. *Frontiers in Microbiology* **12**:735815 DOI [10.3389/fmicb.2021.735815](https://doi.org/10.3389/fmicb.2021.735815).

IUCN. 2022. The IUCN red list of threatened species. Version 2022. Available at <https://www.iucnredlist.org> (accessed 7 November 2023).

Jetz W, Pyron RA. 2018. The interplay of past diversification and evolutionary isolation with present imperilment across the amphibian tree of life. *Nature Ecology & Evolution*: 1. Available at <https://www.nature.com/articles/s41559-018-0515-5> (accessed 1 March 2024).

Johnson PTJ, Buller ID. 2011. Parasite competition hidden by correlated coinfection: using surveys and experiments to understand parasite interactions. *Ecology* **92**(3):535–541 DOI [10.1890/10-0570.1](https://doi.org/10.1890/10-0570.1).

Jones M, Armién A, Rothermel B, Pessier A. 2012. Granulomatous myositis associated with a novel alveolate pathogen in an adult southern leopard frog (*Lithobates sphenocephalus*). *Diseases of Aquatic Organisms* **102**(2):163–167 DOI [10.3354/dao02539](https://doi.org/10.3354/dao02539).

Karwacki EE, Atkinson MS, Ossiboff RJ, Savage AE. 2018. Novel quantitative PCR assay specific for the emerging *Perkinsea* amphibian pathogen reveals seasonal infection dynamics. *Diseases of Aquatic Organisms* **129**(2):85–98 DOI [10.3354/dao03239](https://doi.org/10.3354/dao03239).

Karwacki EE, Martin KR, Savage AE. 2021. One hundred years of infection with three global pathogens in frog populations of Florida, USA. *Biological Conservation* 257:109088 DOI 10.1016/j.biocon.2021.109088.

Kassambara A. 2023. Rstatix: pipe-friendly framework for basic statistical tests. R Package Version 0.7.2. Available at <https://CRAN.R-project.org/package=rstatix>.

Koo MS, Vredenburg VT, Deck JB, Olson DH, Ronnenberg KL, Wake DB. 2021. Tracking, synthesizing, and sharing global *Batrachochytrium* data at AmphibianDisease.org. *Frontiers in Veterinary Science* 8:728232 DOI 10.3389/fvets.2021.728232.

Kriger KM, Pereoglou F, Hero J. 2007. Latitudinal variation in the prevalence and intensity of chytrid (*Batrachochytrium dendrobatidis*) infection in Eastern Australia. *Conservation Biology* 21(5):1280–1290 DOI 10.1111/j.1523-1739.2007.00777.x.

Kuhn M. 2008. Building predictive models in R using the caret package. *Journal of Statistical Software* 28(5):1–26 DOI 10.18637/jss.v028.i05.

Landsberg J, Kiryu Y, Tabuchi M, Waltzek T, Enge K, Reintjes-Tolen S, Preston A, Pessier A. 2013. Co-infection by alveolate parasites and frog virus 3-like *ranavirus* during an amphibian larval mortality event in Florida, USA. *Diseases of Aquatic Organisms* 105(2):89–99 DOI 10.3354/dao02625.

Li Z, Wang Q, Sun K, Feng J. 2021. Prevalence of *Batrachochytrium dendrobatidis* in amphibians from 2000 to 2021: a global systematic review and meta-analysis. *Frontiers in Veterinary Science* 8:791237 DOI 10.3389/fvets.2021.791237.

Liaw A, Wiener M. 2002. Classification and regression by randomForest. *R News* 2:18–22.

Lindauer AL, Maler PA, Voyles J. 2020. Daily fluctuating temperatures decrease growth and reproduction rate of a lethal amphibian fungal pathogen in culture. *BMC Ecology* 20(1):18 DOI 10.1186/s12898-020-00286-7.

Lips KR. 2016. Overview of chytrid emergence and impacts on amphibians. *Philosophical Transactions of the Royal Society B: Biological Sciences* 371(1709):20150465 DOI 10.1098/rstb.2015.0465.

Longcore JR, Longcore JE, Pessier AP, Halteman WA. 2007. Chytridiomycosis widespread in anurans of northeastern United States. *The Journal of Wildlife Management* 71(2):435–444 DOI 10.2193/2006-345.

Longcore JE, Pessier AP, Nichols DK. 1999. *Batrachochytrium dendrobatidis* gen. et sp. nov., a chytrid pathogenic to amphibians. *Mycologia* 91(2):219–227 DOI 10.1080/00275514.1999.12061011.

Longo AV, Lips KR, Zamudio KR. 2023. Evolutionary ecology of host competence after a chytrid outbreak in a naive amphibian community. *Philosophical Transactions of the Royal Society B: Biological Sciences* 378(1882):20220130 DOI 10.1098/rstb.2022.0130.

Luedtke JA, Chanson J, Neam K, Hobin L, Maciel AO, Catenazzi A, Borzée Aël, Hamidy A, Aowphol A, Jean A, Sosa-Bartuano Ál, Fong GA, de Silva A, Fouquet A, Angulo A, Kidov AA, Muñoz Saravia A, Diesmos AC, Tominaga A, Shrestha B, Gratwickie B, Tjaturadi B, Martínez Rivera CC, Vásquez Almazán CR, Señaris C, Chandramouli SR, Strüssmann C, Cortez Fernández CF, Azat C, Hoskin CJ, Hilton-Taylor C, Whyte DL, Gower DJ, Olson DH, Cisneros-Heredia DF, Santana DJ, Nagombi E, Najafi-Majd E, Quah ESH, Bolaños F, Xie F, Brusquetti F, Álvarez FS, Andreone F, Glaw F, Castañeda FE, Kraus F, Parra-Olea G, Chaves G, Medina-Rangel GF, González-Durán G, Ortega-Andrade HM, Machado IF, Das I, Dias IR, Urbina-Cardona JN, Crnobrnja-Isailović J, Yang J-H, Jianping J, Wangyal JT, Rowley JJL, Measey J, Vasudevan K, Chan KO, Gururaja KV, Ovaska K, Warr LC, Canseco-Márquez L, Toledo LF, Díaz LM, Khan MMH,

Meegaskumbura M, Acevedo ME, Napoli MF, Ponce MA, Vaira M, Lampo M, Yáñez-Muñoz MH, Scherz MD, Rödel M-O, Matsui M, Fildor M, Kusrini MD, Ahmed MF, Rais M, Kouamé N'Goran G, García N, Gonwouo NL, Burrowes PA, Imbun PY, Wagner P, Kok PJR, Joglar RL, Auguste RJ, Brandão RA, Ibáñez R, von May R, Hedges SB, Biju SD, Ganesh SR, Wren S, Das S, Flechas SV, Ashpole SL, Robleto-Hernández SJ, Loader SP, Incháustegui SJ, Garg S, Phimmachak S, Richards SJ, Slimani T, Osborne-Naikatini T, Abreu-Jardim TPF, Condez TH, De Carvalho TR, Cutajar TP, Pierson TW, Nguyen TQ, Kaya U, Yuan Z, Long B, Langhammer P, Stuart SN. 2023. Ongoing declines for the world's amphibians in the face of emerging threats. *Nature* 622(7982):308–314 DOI 10.1038/s41586-023-06578-4.

Midwest Association of Fish and Wildlife Agencies (MAFWA). 2020. Missouri 2020 wildlife disease status update. Missouri Department of Conservation Wildlife Health Program. Available at https://www.mafwa.org/wp-content/uploads/2020/11/Part3_7.pdf.

Miller DAW, Grant EHC, Muths E, Amburgey SM, Adams MJ, Joseph MB, Waddle JH, Johnson PTJ, Ryan ME, Schmidt BR, Calhoun DL, Davis CL, Fisher RN, Green DM, Hossack BR, Rittenhouse TAG, Walls SC, Bailey LL, Cruickshank SS, Fellers GM, Gorman TA, Haas CA, Hughson W, Pilliod DS, Price SJ, Ray AM, Sadinski W, Saenz D, Barichivich WJ, Brand A, Brehme CS, Dagit R, Delaney KS, Glorioso BM, Kats LB, Kleeman PM, Pearl CA, Rochester CJ, Riley SPD, Roth M, Sigafus BH. 2018. Quantifying climate sensitivity and climate-driven change in North American amphibian communities. *Nature Communications* 9(1):3926 DOI 10.1038/s41467-018-06157-6.

Miller D, Gray M, Storfer A. 2011. Ecopathology of *Ranaviruses* infecting amphibians. *Viruses* 3(11):2351–2373 DOI 10.3390/v3112351.

Murray KA, Skerratt LF, Garland S, Kriticos D, McCallum H. 2013. Whether the weather drives patterns of endemic amphibian chytridiomycosis: a pathogen proliferation approach. *PLOS ONE* 8(4):e61061 DOI 10.1371/journal.pone.0061061.

O'Brien C, Van Riper C, Myers DE. 2009. Making reliable decisions in the study of wildlife diseases: using hypothesis tests, statistical power, and observed effects. *Journal of Wildlife Diseases* 45(3):700–712 DOI 10.7589/0090-3558-45.3.700.

Olson DH, Aanensen DM, Ronnenberg KL, Powell CI, Walker SF, Bielby J, Garner TWJ, Weaver G, The Bd Mapping Group, Fisher MC. 2013. Mapping the global emergence of *Batrachochytrium dendrobatidis*, the amphibian chytrid fungus. *PLOS ONE* 8(2):e56802 DOI 10.1371/journal.pone.0056802.

Olson DH, Ronnenberg KL, Glidden CK, Christiansen KR, Blaustein AR. 2021. Global patterns of the fungal pathogen *Batrachochytrium dendrobatidis* support conservation urgency. *Frontiers in Veterinary Science* 8:685877 DOI 10.3389/fvets.2021.685877.

Petersen CE, Lovich RE, Phillips CA, Dreslik MJ, Lannoo MJ. 2016. Prevalence and seasonality of the amphibian chytrid fungus *Batrachochytrium dendrobatidis* along widely separated longitudes across the United States. *EcoHealth* 13(2):368–382 DOI 10.1007/s10393-016-1101-4.

Peterson AC, McKenzie VJ. 2014. Investigating differences across host species and scales to explain the distribution of the amphibian pathogen *Batrachochytrium dendrobatidis*. *PLOS ONE* 9(9):e107441 DOI 10.1371/journal.pone.0107441.

Price SJ, Leung WTM, Owen CJ, Puschendorf R, Sergeant C, Cunningham AA, Balloux F, Garner TWJ, Nichols RA. 2019. Effects of historic and projected climate change on the range and impacts of an emerging wildlife disease. *Global Change Biology* 25(8):2648–2660 DOI 10.1111/gcb.14651.

R Core Team. 2023. *R: a language and environment for statistical computing*. Vienna, Austria: R Foundation for Statistical Computing. Available at <https://www.R-project.org/>.

Raffel TR, Halstead NT, McMahon TA, Davis AK, Rohr JR. 2015. Temperature variability and moisture synergistically interact to exacerbate an epizootic disease. *Proceedings of the Royal Society B: Biological Sciences* **282**(1801):20142039 DOI [10.1098/rspb.2014.2039](https://doi.org/10.1098/rspb.2014.2039).

Raffel TR, Rohr JR, Kiesecker JM, Hudson PJ. 2006. Negative effects of changing temperature on amphibian immunity under field conditions. *Functional Ecology* **20**(5):819–828 DOI [10.1111/j.1365-2435.2006.01159.x](https://doi.org/10.1111/j.1365-2435.2006.01159.x).

Raffel TR, Romansic JM, Halstead NT, McMahon TA, Venesky MD, Rohr JR. 2013. Disease and thermal acclimation in a more variable and unpredictable climate. *Nature Climate Change* **3**(2):146–151 DOI [10.1038/nclimate1659](https://doi.org/10.1038/nclimate1659).

Rambaut A. 2010. FigTree v1.3.1. Institute of Evolutionary Biology, University of Edinburgh, Edinburgh. Available at <http://tree.bio.ed.ac.uk/software/figtree> (accessed 1 March 2024).

Ramsay C, Rohr JR. 2021. The application of community ecology theory to co-infections in wildlife hosts. *Ecology* **102**(3):e03253 DOI [10.1002/ecy.3253](https://doi.org/10.1002/ecy.3253).

Rödder D, Schulte U, Toledo LF. 2013. High environmental niche overlap between the fungus *Batrachochytrium dendrobatidis* and invasive bullfrogs (*Lithobates catesbeianus*) enhance the potential of disease transmission in the Americas. *North-Western Journal of Zoology* **9**(1):178–184.

Rollins-Smith LA. 1998. Metamorphosis and the amphibian immune system. *Immunological Reviews* **166**(1):221–230 DOI [10.1111/j.1600-065x.1998.tb01265.x](https://doi.org/10.1111/j.1600-065x.1998.tb01265.x).

Rollins-Smith LA. 2017. Amphibian immunity-stress, disease, and climate change. *Developmental & Comparative Immunology* **66**(2):111–119 DOI [10.1016/j.dci.2016.07.002](https://doi.org/10.1016/j.dci.2016.07.002).

Rollins-Smith LA. 2020. Global amphibian declines, disease, and the ongoing battle between *Batrachochytrium* fungi and the immune system. *Herpetologica* **76**(2):178–188 DOI [10.1655/0018-0831-76.2.178](https://doi.org/10.1655/0018-0831-76.2.178).

Roth SA, Griffis-Kyle KL, Barnes MA. 2024. *Batrachochytrium dendrobatidis* in the arid and thermally extreme Sonoran Desert. *EcoHealth* **20**(4):370–380 DOI [10.1007/s10393-023-01668-1](https://doi.org/10.1007/s10393-023-01668-1).

Rothermel B, Miller D, Travis E, Gonynor McGuire J, Jensen J, Yabsley M. 2016. Disease dynamics of red-spotted newts and their anuran prey in a montane pond community. *Diseases of Aquatic Organisms* **118**(2):113–127 DOI [10.3354/dao02965](https://doi.org/10.3354/dao02965).

Sasso T, McCallum H, Grogan L. 2021. Occurrence of *Batrachochytrium dendrobatidis* within and between species: a review of influential variables as identified from field studies. *Biological Conservation* **262**(1795):109300 DOI [10.1016/j.biocon.2021.109300](https://doi.org/10.1016/j.biocon.2021.109300).

Savage AE, Becker CG, Zamudio KR. 2015. Linking genetic and environmental factors in amphibian disease risk. *Evolutionary Applications* **8**(6):560–572 DOI [10.1111/eva.12264](https://doi.org/10.1111/eva.12264).

Savage AE, Muletz-Wolz CR, Campbell Grant EH, Fleischer RC, Mulder KP. 2019. Functional variation at an expressed MHC class II β locus associates with *Ranavirus* infection intensity in larval anuran populations. *Immunogenetics* **71**(4):335–346 DOI [10.1007/s00251-019-01104-1](https://doi.org/10.1007/s00251-019-01104-1).

Savage AE, Sredl MJ, Zamudio KR. 2011. Disease dynamics vary spatially and temporally in a North American amphibian. *Biological Conservation* **144**(6):1910–1915 DOI [10.1016/j.biocon.2011.03.018](https://doi.org/10.1016/j.biocon.2011.03.018).

Scheele BC, Pasmans F, Skerratt LF, Berger L, Martel A, Beukema W, Acevedo AA, Burrowes PA, Carvalho T, Catenazzi A, De la Riva I, Fisher MC, Flechas SV, Foster CN, Frias-Álvarez P, Garner TWJ, Gratwicke B, Guayasamin JM, Hirschfeld M, Kolby JE, Kosch TA, La Marca E, Lindenmayer DB, Lips KR, Longo AV, Maneyro R, McDonald CA, Mendelson J III, Palacios-Rodriguez P, Parra-Olea G, Richards-Zawacki CL, Rödel M-O, Rovito SM, Soto-Azat C, Toledo LF, Voyles J, Weldon C, Whittfield SM, Wilkinson M,

Zamudio KR, Canessa S. 2019. Amphibian fungal panzootic causes catastrophic and ongoing loss of biodiversity. *Science* **363**(6434):1459–1463 DOI [10.1126/science.aav0379](https://doi.org/10.1126/science.aav0379).

Schwalbe N, Wahl B. 2020. Artificial intelligence and the future of global health. *The Lancet* **395**(10236):1579–1586 DOI [10.1016/S0140-6736\(20\)30226-9](https://doi.org/10.1016/S0140-6736(20)30226-9).

Smith KF, Acevedo-Whitehouse K, Pedersen AB. 2009. The role of infectious diseases in biological conservation. *Animal Conservation* **12**(1):1–12 DOI [10.1111/j.1469-1795.2008.00228.x](https://doi.org/10.1111/j.1469-1795.2008.00228.x).

Sonn JM, Utz RM, Richards-Zawacki CL. 2019. Effects of latitudinal, seasonal, and daily temperature variations on chytrid fungal infections in a North American frog. *Ecosphere* **10**(11):e02892 DOI [10.1002/ecs2.2892](https://doi.org/10.1002/ecs2.2892).

Stallknecht DE. 2007. Impediments to wildlife disease surveillance, research, and diagnostics. In: Childs JE, Mackenzie JS, Richt JA, eds. *Wildlife and Emerging Zoonotic Diseases: The Biology, Circumstances and Consequences of Cross-Species Transmission*. Berlin, Heidelberg: Springer, 445–461.

Sundar D. 2006. binom: binomial confidence intervals for several parameterizations. Version 1.1 DOI [10.32614/CRAN.package.binom](https://doi.org/10.32614/CRAN.package.binom).

Teacher AGF, Cunningham AA, Garner TWJ. 2010. Assessing the long-term impact of *Ranavirus* infection in wild common frog populations. *Animal Conservation* **13**(5):514–522 DOI [10.1111/j.1469-1795.2010.00373.x](https://doi.org/10.1111/j.1469-1795.2010.00373.x).

Thompson CW, Phelps KL, Allard MW, Cook JA, Dunnum JL, Ferguson AW, Gelang M, Khan FAA, Paul DL, Reeder DM, Simmons NB, Vanhove MPM, Webala PW, Weksler M, Kilpatrick CW. 2021. Preserve a voucher specimen! The critical need for integrating natural history collections in infectious disease studies. *mBio* **12**(1):e02698-20 DOI [10.1128/mBio.02698-20](https://doi.org/10.1128/mBio.02698-20).

Torres López AS, Wiley DLF, Omlor KN, Eberle CM, Barrow LN. 2024. Dynamics of amphibian pathogen detection using extended museum specimens. *Journal of Wildlife Diseases* **60**(4):1004–1010 DOI [10.7589/JWD-D-24-00025](https://doi.org/10.7589/JWD-D-24-00025).

Trujillo AL, Hoffman EA, Becker CG, Savage AE. 2021. Spatiotemporal adaptive evolution of an MHC immune gene in a frog-fungus disease system. *Heredity* **126**(4):640–655 DOI [10.1038/s41437-020-00402-9](https://doi.org/10.1038/s41437-020-00402-9).

Vredenburg VT, Knapp RA, Tunstall TS, Briggs CJ. 2010. Dynamics of an emerging disease drive large-scale amphibian population extinctions. *Proceedings of the National Academy of Sciences of the United States of America* **107**(21):9689–9694 DOI [10.1073/pnas.0914111107](https://doi.org/10.1073/pnas.0914111107).

Whitfield S, Alvarado G, Abarca J, Zumbado H, Zuñiga I, Wainwright M, Kerby J. 2017. Differential patterns of *Batrachochytrium dendrobatidis* infection in relict amphibian populations following severe disease-associated declines. *Diseases of Aquatic Organisms* **126**(1):33–41 DOI [10.3354/dao03154](https://doi.org/10.3354/dao03154).

Wickham H. 2016. *Ggplot2*. Cham: Springer International Publishing.

Wilkinson MD, Dumontier M, Aalbersberg IJJ, Appleton G, Axton M, Baak A, Blomberg N, Boiten JW, da Silva Santos LB, Bourne PE, Bouwman J, Brookes AJ, Clark T, Crosas M, Dillo I, Dumon O, Edmunds S, Evelo CT, Finkers R, Gonzalez-Beltran A, Gray AJG, Groth P, Goble C, Grethe JS, Heringa J, 't Hoen PAC, Hooft R, Kuhn T, Kok R, Kok J, Lusher SJ, Martone ME, Mons A, Packer AL, Persson B, Rocca-Serra P, Roos M, van Schaik R, Sansone S-A, Schultes E, Sengstag T, Slater T, Strawn G, Swertz MA, Thompson M, van der Lei J, van Mulligen E, Velterop J, Waagmeester A, Wittenburg P, Wolstencroft K, Zhao J, Mons B. 2016. The FAIR guiding principles for scientific data management and stewardship. *Scientific Data* **3**:160018 DOI [10.1038/sdata.2016.18](https://doi.org/10.1038/sdata.2016.18).

Woodhams DC, Ardipradja K, Alford RA, Marantelli G, Reinert LK, Rollins-Smith LA. 2007. Resistance to chytridiomycosis varies among amphibian species and is correlated with skin peptide defenses. *Animal Conservation* **10**(4):409–417 DOI [10.1111/j.1469-1795.2007.00130.x](https://doi.org/10.1111/j.1469-1795.2007.00130.x).

World Organisation for Animal Health (WOAH). 2021a. Manual of diagnostic tests for aquatic animals: Chapter 2.1.1.—infection with *Batrachochytrium dendrobatidis*. Manual of Diagnostic Tests for Aquatic Animals. Available at https://www.woah.org/fileadmin/Home/eng/Health_standards/aahm/current/2.1.01_Bdendro.pdf.

World Organisation for Animal Health (WOAH). 2021b. Infection with *Ranavirus*. In: *Manual of Diagnostic Tests for Aquatic Animals*. Available at https://www.woah.org/fileadmin/Home/eng/Health_standards/aahm/current/2.1.03_RANAVIRUS.pdf (Accessed March 2024).

Xie GY, Olson DH, Blaustein AR. 2016. Projecting the global distribution of the emerging amphibian fungal pathogen, *Batrachochytrium dendrobatidis*, based on IPCC climate futures. *PLOS ONE* **11**(8):e0160746 DOI [10.1371/journal.pone.0160746](https://doi.org/10.1371/journal.pone.0160746).

Yap TA, Koo MS, Ambrose RF, Vredenburg VT. 2018. Introduced bullfrog facilitates pathogen invasion in the western United States. *PLOS ONE* **13**(4):e0188384 DOI [10.1371/journal.pone.0188384](https://doi.org/10.1371/journal.pone.0188384).

Youker-Smith TE, Boersch-Supan PH, Whippes CM, Ryan SJ. 2018. Environmental drivers of *Ranavirus* in free-living amphibians in constructed ponds. *EcoHealth* **15**(3):608–618 DOI [10.1007/s10393-018-1350-5](https://doi.org/10.1007/s10393-018-1350-5).